Journal of Experimental Botany, Vol. 72, No. 12 pp. 4548–4564, 2021
doi:10.1093/jxb/erab140 Advance Access Publication 27 March 2021

RESEARCH PAPER

Induction of *S*-nitrosoglutathione reductase protects root growth from ammonium toxicity by regulating potassium homeostasis in Arabidopsis and rice

Lin Zhang[1,*], Haiyan Song[2,*], Baohai Li[3], Meng Wang[1], Dongwei Di[1], Xianyong Lin[3], Herbert J. Kronzucker[4,5], Weiming Shi[1], and Guangjie Li[1,†]

[1] State Key Laboratory of Soil and Sustainable Agriculture, Institute of Soil Science, Chinese Academy of Sciences, No. 71 East Beijing Road, Nanjing 210008, China
[2] Academic Affairs Office, Foshan University, Foshan, China
[3] MOE Key Laboratory of Environment Remediation and Ecological Health, College of Environmental & Resource Sciences, Zhejiang University, Hangzhou, 310058, China
[4] Faculty of Land and Food Systems, University of British Columbia, Vancouver, BC, V6T 1Z4 Canada
[5] School of BioSciences, The University of Melbourne, Parkville, Victoria 3010, Australia

* These authors contributed equally to this work.
† Correspondence: gjli@issas.ac.cn

Received 9 December 2020; Editorial decision 23 March 2021; Accepted 24 March 2021

Editor: Ann Cuypers, Hasselt University, Belgium

Abstract

Ammonium (NH_4^+) is toxic to root growth in most plants already at moderate levels of supply, but mechanisms of root growth tolerance to NH_4^+ remain poorly understood. Here, we report that high levels of NH_4^+ induce nitric oxide (NO) accumulation, while inhibiting potassium (K^+) acquisition via SNO1 (sensitive to nitric oxide 1)/SOS4 (salt overly sensitive 4), leading to the arrest of primary root growth. High levels of NH_4^+ also stimulated the accumulation of GSNOR (*S*-nitrosoglutathione reductase) in roots. GSNOR overexpression improved root tolerance to NH_4^+. Loss of GSNOR further induced NO accumulation, increased SNO1/SOS4 activity, and reduced K^+ levels in root tissue, enhancing root growth sensitivity to NH_4^+. Moreover, the GSNOR-like gene, *OsGSNOR*, is also required for NH_4^+ tolerance in rice. Immunoblotting showed that the NH_4^+-induced GSNOR protein accumulation was abolished in the VTC1- (vitamin C1) defective mutant *vtc1-1*, which is hypersensititive to NH_4^+ toxicity. GSNOR overexpression enhanced *vtc1-1* root tolerance to NH_4^+. Our findings suggest that induction of GSNOR increases NH_4^+ tolerance in Arabidopsis roots by counteracting NO-mediated suppression of tissue K^+, which depends on VTC1 function.

Keywords: Ammonium stress, nitric oxide, potassium, root growth, *S*-nitrosoglutathione reductase (GSNOR), vitamin C1 (VTC1).

Introduction

Ammonium (NH_4^+) would be expected to be a preferred source of nitrogen (N) for plants, given that its uptake is less energetically demanding than that of nitrate (NO_3^-) and that it does not require reduction prior to incorporation into amino acids and proteins (Glass *et al.*, 1997; Xu *et al.*, 2012; Krapp, 2015; Wu *et al.*, 2019). Also, N losses from agricultural fields, a growing environmental threat (Coskun *et al.*, 2017b, c), tend to be greatly lessened when NH_4^+- rather than NO_3^--based fertilizers are employed (Coskun *et al.*, 2017c). Ammonium-based fertilizers, formulated together with nitrification inhibitors, have been shown to be useful in mitigating the detrimental effects of N leaching and run-off from agricultural fields into natural water bodies under a variety of circumstances (Coskun *et al.*, 2017c; Torralbo *et al.*, 2017; Lu *et al.*, 2019; Wang and Li, 2019; Min *et al.*, 2021). Therefore, a deeper study of the mechanisms of plant N source preference is urgently required. For most plant species, however, NH_4^+, despite these energetic and ecosystem-level advantages, represents a stressor even at moderate levels, and generally occurs as external NH_4^+ concentrations rise above 0.1–0.5 mmol l^{-1} (Britto and Kronzucker, 2002, 2013). Because the root is the first organ to encounter and sense soil stresses (Walker *et al.*, 2017), the initial, direct effects of NH_4^+ on modulating root system growth are of particular importance (Li *et al.*, 2014). Indeed, a stunted root system, especially the inhibition of primary root growth, is a near-universal symptom of NH_4^+ sensitivity (Britto and Kronzucker, 2002; Li *et al.*, 2010; Zheng *et al.*, 2015; Straub *et al.*, 2017), but the mechanisms behind this are still insufficiently resolved (see the reviews of Kronzucker *et al.*, 2001, Britto and Kronzucker, 2002, Li *et al.*, 2014, and Liu and von Wirén, 2017). Elucidating the mechanisms by which NH_4^+ inhibits root growth is pivotal to understanding the adaptation and acclimation of root system architecture to NH_4^+ stress (Lay-Pruitt and Takahashi, 2020).

Several important physiological processes have been linked to excessive NH_4^+ exposure, such as relationships with carbon biochemistry, energy consumption, and modifications of hormonal balance (Britto and Kronzucker, 2002). One particularly well-documented effect of NH_4^+ is that of disruption of cation nutrition, especially that of K^+ (Szczerba *et al.*, 2008a; Li *et al.*, 2014; Bittsánszky *et al.*, 2015), an effect whose reciprocity entails K^+ alleviation of NH_4^+ toxicity (Szczerba *et al.*, 2008*b*; Balkos *et al.*, 2010; Coskun *et al.*, 2017a). However, the molecular mechanisms by which NH_4^+ affects K^+ homeostasis, or of how K^+ may alleviate NH_4^+ toxicity, except for direct effects on primary membrane transport (Szczerba *et al.*, 2008a, *b*; Coskun *et al.*, 2017a) and resultant effects on tissue ion accumulation (Britto and Kronzucker, 2002), are only partially understood. Nitric oxide (NO) is a signal molecule with a plethora of biological functions in plants (Besson-Bard *et al.*, 2008; Shi *et al.*, 2012; Frungillo *et al.*, 2014, including important roles in the regulation of root growth and development. Recent studies have shown that NO is an important component of root growth acclimation to a variety of stresses, such as cadmium (Cd) toxicity, copper (Cu) excess, iron (Fe) deficiency, and aluminum (Al) toxicity (Neill *et al.*, 2003; Crawford and Guo, 2005; Tian *et al.*, 2007; Peto *et al.*, 2013; Alemayehu *et al.*, 2015; Zhang *et al.*, 2018). Recently, NO production has also been reported to increase under NH_4^+ treatment conditions (Hachiya and Noguchi, 2011; Wang *et al.*, 2011). Thus, it can be speculated that there may be a relationship between NO and the plant response to NH_4^+. The biosynthesis of NO can proceed via several enzymatic and non-enzymatic reactions, depending on the site and the nature of the stimulus for NO production (Gupta *et al.*, 2011; Yu *et al.*, 2014). The NO synthase (NOS) enzyme is the major pathway for NO production in animals, while no typical NOS sequences have been found in 1087 sequenced transcriptomes of land plants; however, sequences have been found in 15 algal species (Jeandroz *et al.*, 2016). The emerging data suggest that plants use nitrate reductase (NR)-mediated nitrate reduction as the major pathway to synthesize NO (Jeandroz *et al.*, 2016; Chamizo-Ampudia *et al.*, 2017). On the other hand, cells possess various mechanisms for removing NO. For example, NO reacts with glutathione (GSH) to form *S*-nitrosoglutathione (GSNO), which is then metabolized by the enzyme GSNO reductase (GSNOR) (Liu *et al.*, 2001; Chaki *et al.*, 2010; Malik *et al.*, 2011; Zhou *et al.*, 2016; Matamoros *et al.*, 2020). GSNOR, encoded by a single-copy gene, shows cytosolic localization in Arabidopsis. GSNOR is involved in several stress responses, and, for example, plays a critical role in both Fe excess and Cd toxicity tolerance of primary root growth in Arabidopsis (Zhang *et al.*, 2018; Guan *et al.*, 2019; Li *et al.*, 2019). The emerging role of GSNOR as a master regulator in oxidative stress more generally, through its regulation of the interaction of reactive oxygen and nitrogen species (ROS/RNS), is also of importance (Li *et al.*, 2021). However, the mechanisms by which the highly conserved GSNOR proteins are regulated are still largely unknown in any organism, especially during the NH_4^+ response. Vitamin C1 (VTC1) is a key genetic determinant of primary root growth NH_4^+ sensitivity (Qin *et al.*, 2008; Li *et al.*, 2010; Kempinski *et al.*, 2011). Barth and co-authors have suggested that NH_4^+ hypersensitivity in the *vtc1-1* mutant may be caused by disturbed NO signaling (Barth *et al.*, 2010). However, this has not been explored further experimentally, and the linkage between stunted primary root growth and NO accumulation in the *vtc1-1* mutant has remained unresolved.

In this study, we employed Arabidopsis Columbia-0 (Col-0) and GSNOR mutants and related transgenic lines to explore the possible mechanism underpinning the root tolerance to NH_4^+, and to elucidate the relationship of VTC1 and GSNOR.

The role of OsGSNOR in the NH_4^+ toxicity tolerance of rice was also tested. The potential mechanisms involved in the stress response to NH_4^+ toxicity are discussed.

Materials and methods

Plant materials and growth conditions

Plant materials used in this work included wild-type (Col-0) *Arabidopsis thaliana* L. and genetic mutants derived from the Col-0 background. *hot5-2/gsnor* (Li *et al.*, 2019), *nia1nia2* (Zhu *et al.*, 2016), *proGSNOR:GSNOR-GFP/hot5-2* (Li *et al.*, 2019), and the overexpression line *VTC1-HA*/Col-0 (Wang *et al.*, 2013) were described previously. The *nox1*, *vtc1-1*, *noa1*, and *sno1/sos4* mutants were obtained from the Arabidopsis Biological Resource Center (ABRC). For overexpression of GSNOR in Col-0 and *vtc1-1*, the full coding sequence of GSNOR was amplified by PCR via specific primers (Supplementary Table S1), using the *Sal*I and *Bam*HI sites, and cloned into pBinGFP4. The resulting plasmids were then separately introduced into Col-0 and *vtc1-1*, and the transgenic lines were confirmed by real-time quantitative PCR (qRT-PCR) amplification. Seeds were surface-sterilized and cold-treated at 4 °C for 48 h prior to being sown onto Petri dishes containing standard growth medium. The Arabidopsis standard growth medium was as described previously (Li *et al.*, 2013) and was composed of 2 mM KH_2PO_4, 5 mM $NaNO_3$, 2 mM $MgSO_4$, 1 mM $CaCl_2$, 50 μM Fe-EDTA, 50 μM H_3BO_3, 12 μM $MnSO_4$, 1 μM $ZnCl_2$, 1 μM $CuSO_4$, 0.2 μM Na_2MoO_4, 1% sucrose, and 0.8% agar (pH 5.7, adjusted with 1 M NaOH). The day of Arabidopsis sowing was considered day 0. Seedlings were grown, oriented vertically on the surface of the vertically oriented Petri dishes (allowing gravity-driven root growth), in a growth chamber set to a 16 h light:8 h dark photoperiod, an irradiance of 100 μmol m^{-2} s^{-1}, and a temperature of 23±1 °C. For NH_4^+ stress experiments ($+NH_4^+$), seedlings were grown in standard medium (Ctrl) containing various concentrations of $(NH_4)_2SO_4$. To study the effect of exogenous cPTIO [2-(4-carboxyphenyl)-4,4,5,5-tetramethylimidazoline-1-oxyl-3-oxide], SNP (sodium nitroprusside), L-NAME (N^G-nitro-L-arginine methyl ester), L-NMME (N^G-monomethyl-L-arginine), and TEA (tetraethylammonium), seedlings were supplemented with or without ammonium plus the indicated concentrations of the added compounds. Rice seeds {Zhonghua 11 (wild type) and OsGSNOR (Os02G57040) CRISPR/Cas9 [clustered regularly interspaced palindromic repeats/CRISPR-associated protein 9] lines, which were described in our previous report (Li *et al.*, 2019)}, were surface-sterilized with 3% H_2O_2 for 20 min, washed with sterile water, soaked in water for 24 h in the dark, and transferred to a nylon net floating on 0.5 mM $CaCl_2$ for 3 d. Then, rice seedlings were transferred to modified Kimura's solution (Ctrl) as follows: 0.5 mM $MgSO_4{\cdot}7H_2O$, 0.5 mM $NaNO_3$, 0.36 mM $CaCl_2{\cdot}2H_2O$, 0.25 mM KCl, 0.2 mM NaH_2PO_4, 9 μM $MnCl_2{\cdot}4H_2O$, 0.5 μM $Na_2MoO_4{\cdot}2H_2O$, 0.3 μM $CuSO_4{\cdot}5H_2O$, 0.7 μM $ZnSO_4{\cdot}7H_2O$, 0.1 mM Fe-EDTA, and 50 μM H_3BO_3; 10 mM NH_4Cl was added in the control as the ammonium treatment ($+NH_4^+$) stress. The rice nutrient solution pH was adjusted to 5.5. Plants were grown in a growth chamber, with a 400 μmol m^{-2} s^{-1} light intensity, 65% relative humidity, and a 16 h (30 °C)/8 h (28 °C) day/night cycle. The nutrient solution was exchanged every 2 d.

Root growth measurements

Primary root lengths of individual Arabidopsis seedlings were directly measured with Image J software from digital images captured with a Canon G7 camera. Rice total root lengths were measured using a root analysis instrument (WinRHIZO; Regent Instruments Inc., Quebec, ON, Canada).

Tissue NH_4^+ and K^+ content assay

The seedlings were grown in medium for 7 d, and then harvested. To determine tissue NH_4^+ content, seedlings were desorbed for 5 min in 10 mM $CaSO_4$ to remove extracellular NH_4^+ according to B.H. Li *et al.* (2012) and Hachiya *et al.* (2012). Considering possible ammonium metabolism and net production, all samples were washed simultaneously to eliminate this potential interference. Then, the samples were weighed and frozen in liquid nitrogen, and subsequently extracted with 1 ml of 10 mM formic acid for the NH_4^+ content assay by HPLC, following derivatization with *o*-phthaldialdehyde, as described previously (G.J. Li *et al.*, 2012). For K^+ content analyses, the samples were washed with 10 mM $CaSO_4$ for 5 min to clear agar and K^+ adhering to the root surface and cell wall apoplast (Britto *et al.*, 2006; Coskun *et al.*, 2010; Han *et al.*, 2016; Shabala *et al.*, 2016) and then dried at 75 °C prior to analysis, and digested with HNO_3. Determination of the potassium in solution was made using a flame photometer (Model HG-5, Beijing detection instrument Ltd), using an internal standard procedure employing 3 mmol l^{-1} lithium chloride.

Root NH_4^+ influx

Root $^{15}NH_4^+$ influx was assayed as described previously (Léran *et al.*, 2015). Briefly, the plants were grown for 7 d on the surface of the vertically oriented Petri dishes with standard growth medium. Plants (~30 seedlings for each replicate) were transferred to 10 mM $CaSO_4$ solution in Petri dishes for 1 min, then roots were transferred to nutrient solution (pH 5.7) containing 10 mM $^{15}NH_4^+$ (20% atom excess ^{15}N) for 30 min, and finally washed in 10 mM $CaSO_4$ for 5 min. The seedlings were dried at 70 °C for at least 48 h. After determination of their dry weight, the samples were analyzed for total nitrogen and atom % ^{15}N using a Euro-EA Euro Vector elemental analyzer coupled with an IsoPrime mass spectrometer (GV Instruments). The total ^{15}N amount was calculated according to the equations of Drescher *et al.* (2020). Total N uptake (g)=%N in sample×DW (g)/100. The % atom ^{15}N in excess in sample=% atom ^{15}N in sample−0.3663% (natural ^{15}N abundance). Total ^{15}N amount (g)=Total N uptake×(% atom ^{15}N in excess in sample/% atom ^{15}N in excess in fertilizer). The formula used in $^{15}NH_4^+$ influx was: total ^{15}N amount/DW/0.5 h, yielding the amount of ^{15}N taken up per unit weight per unit time.

Measurement of net K^+ flux with the non-invasive micro-test (NMT) system

Net fluxes of K^+ were measured non-invasively from the root mature zone (~2500 μm from the tip of roots) using the NMT technique (NMT system BIO-IM; Younger USA, LLC, Amherst, MA, USA). The principle of the method and the instrument are detailed in Li *et al.* (2010). Briefly, Arabidopsis seedlings were grown in a Petri dish for 7 d, and then transferred to growth medium with or without 10 mM NH_4^+ for 24 h. For pre-treatments, plants were pre-treated with mock solution with or without 10 mM NH_4^+ for 1 h. After the specified pre-treatment duration, the pre-treatment solution was withdrawn and the measuring solution with 1 mM K^+ and 10 mM NH_4^+ was introduced. For each treatment, at least five plants were used for K^+ flux analyses. All measurements of net K^+ fluxes were carried out at Xuyue Science and Technology Co. Ltd (Beijing, China).

Measurement of NO production

The endogenous NO level was visualized using an NO-specific fluorescent probe DAF-FM DA (3-amino,4-aminomethyl-2′,7′-difluorescein, diacetate) (5 μM), according to the method of Wang *et al.* (2014), with some modifications. The NO fluorescence intensity was determined by

calculating the relative contribution of the green channel using the values of the RGB color model in Photoshop 7.0 (Adobe Systems Inc., San Jose, CA, USA). According to Barth *et al.* (2010), NO content (as nitrite) was determined using the micro NO content assay kit (BC1475, Solarbio, Beijing) in accordance with the manufacturer's recommendations in seedlings. NO content was calculated by comparison with a standard curve of $NaNO_2$.

Activity analyses of NR, NOS, and SNO1/SOS4

The NR activity in roots was detected by a micro NR assay kit (NR-1-Y, Suzhou Keming Biotechnology Co., Ltd, Suzhou, China), according to the manufacturer's recommendations. This kit functions by assaying how NR catalyzes the reduction of nitrate to nitrite according to the reaction: $NO_3^-+NADH+H^+ \rightarrow NO_2^-+NAD^++H_2O$. The NOS activity was detected by a total NOS assay kit (A014-2, Nanjing Jiancheng Bioengineering Institute, Nanjing, China), according to the manufacturer's recommendations. This kit functions by assaying NOS catalytic ability of the reaction between molecular oxygen and L-Arg to generate NO; NO then reacted with a nucleophilic substance to form a colored compound, measured at 530 nm, and the activity of NOS was calculated according to absorbance. The SNO1 (sensitive to nitric oxide 1)/SOS4 (salt overly sensitive 4) activity was measured according to Xia *et al.* (2014), by using a colorimetric procedure. Briefly, 0.5 ml of crude extract (containing 1–7 mg of total protein) was used in a buffer containing 0.1 mM $ZnCl_2$, 0.2 mM ATP, 0.2 mM pyridoxal, and 70 mM K_3PO_4. At 37 °C, reactions were stopped by addition of 50 ml of chilled 50% trichloroacetic acid (TCA; w/v) after a 1 h incubation. Protein was pelleted by centrifugation (1500 *g*) at 4 °C for 10 min. Then the supernatant was transferred to another clean tube. After the addition of 2% phenylhydrazine (in 10 N H_2SO_4) and incubation on ice for 30 min, the pyridoxal 5′-phosphate formation was measured based on the absorbance at 410 nm.

qRT-PCR analysis

Total RNA was extracted from Arabidopsis roots. The samples of independent biological replicates were individually ground to a powder in liquid nitrogen, and total RNA was isolated using the EASY-spin plant RNA kit (Aidlab, Beijing, China), according to the manufacturer's instructions. Total RNA quality and quantity were analyzed by a NanoPhotometer® spectrophotometer (Implen, Health Care Facilities & Svcs, La Baya Drive West Lake, CA, USA), and RNA degradation and contamination were checked on a 1% agarose electrophoresis gel. For qRT-PCR, the total cDNA was synthesized using HiScript II RT SuperMix (Vazyme, Nanjing, China) according to the manufacturer's instructions. The cDNAs were then used as templates for qPCR with gene-specific primers. Gene-specific primers for qRT-PCR were designed using Primer-5 software. The primers are presented in the Table. S1. The qRT-PCR assays were performed using the LightCycler 480 II real-time PCR device with specific primers (Roche, Sweden) and Lightcycler 480 SYBR Green (Roche, Sweden). *ACTIN2* was used as the internal reference gene, and relative RNA abundance was normalized to the *ACTIN2* internal control ($[mRNA]_{gene}/[mRNA]_{ACTIN2}$). The expression level of the *ACTIN2* gene was similar among different samples, with the same initial amount of RNA for reverse transcription (Supplementary Fig. S8). *CBP20*, encoding nuclear cap-binding protein, was also used as a reference gene (Li *et al.*, 2013) for qRT-PCR analysis in Supplementary Figs S9 and S10. Three biological replicates were performed for each sample, and three technical replicates were also included for each biological replicate. The $2^{-\Delta\Delta ct}$ method with three biological replicates was employed to analyze the expression levels.

Western blotting

Arabidopsis proteins were extracted from 7-day-old seedling roots that were treated with or without varying concentrations of NH_4^+. Protein concentration was determined by the bicinchoninic acid (BCA) method. An aliquot (12.5 μg protein per lane) of the total protein was separated by 12% SDS–PAGE and blotted onto a PVDF membrane. GSNOR [1:1000, AS09647; Agrisera, Vännäs, Sweden; according to Zhou *et al.* (2016)] and anti-HA (1:1000, AT0079; Engibody Biotechnology, USA) primary antibodies, and subsequently a sheep anti-rabbit IgG H&L horseradish peroxidase-conjugated antibody (1:5000; Abcam) were used for western blot analyses.

Immunoprecipitation MS (IP-MS) analysis

The transgenic line that contains the GSNOR gene with a green fluorescent protein (GFP) tag driven by the native promoter in a *hot5-2/gsnor* background was used for protein IP followed by MS. GFP antibody-pre-connected agarose beads (Sigma) were used for enrichment of GFP and candidate interacting proteins. The digested peptides were vacuum-dried, redissolved and desalted, and separated on a reverse-phase column (Ultimate RSLCnano 3000; ThermoFisher Scientific), coupled online to an LTQ-XL linear ion-trap mass spectrometer (ThermoFisher Scientific).

Statistical and graphical analyses

The data were statistically analyzed using the SPSS 13.0 program (SPSS Chicago, IL, USA) for all experiments. Details are shown in the figure legends. Graphs were produced using Origin 8.0.

Accession numbers

ACTIN2 (At3g18780), *CAM1* (At5g37780), *CAM4* (At1g66410), *CBP20* (At5g44200), *GSNOR* (At5g43940), *NIA1* (At1g77760), *NIA2* (At1g37130), *VTC1* (At2g39770), and *OsGSNOR* (Os02g57040)

Results

Ammonium affects root growth through the accumulation of NO

Staining roots *in situ* with an NO-specific dye showed that NH_4^+ stimulated NO accumulation in wild-type (Col-0) roots (Fig. 1A, B), and this result was confirmed by estimating NO (as nitrite) content (Fig. 1C), according to the method of Barth *et al.* (2010). To investigate the possible role of NO in NH_4^+ inhibition of root growth, we first investigated the effects of cPTIO (a widely used NO scavenger) and SNP (an NO donor) on root growth under NH_4^+. Application of cPTIO clearly reversed the decrease in the rate of primary root growth compared with NH_4^+ treatment alone (Fig. 1D). However, the application of SNP clearly enhanced NH_4^+ inhibition of root growth (Fig. 1E). To validate our results, we tested the response of a mutant with high levels of endogenous NO using the NO-overproducing mutant *nox1* to NH_4^+. The *nox1* mutant was found to be significantly more sensitive to NH_4^+ than Col-0, and primary root growth was ~18% for *nox1*, while it was ~56% for Col-0 compared with the respective controls (Fig. 1F, G). The results suggest that increased NO content is involved in NH_4^+ inhibition of root growth.

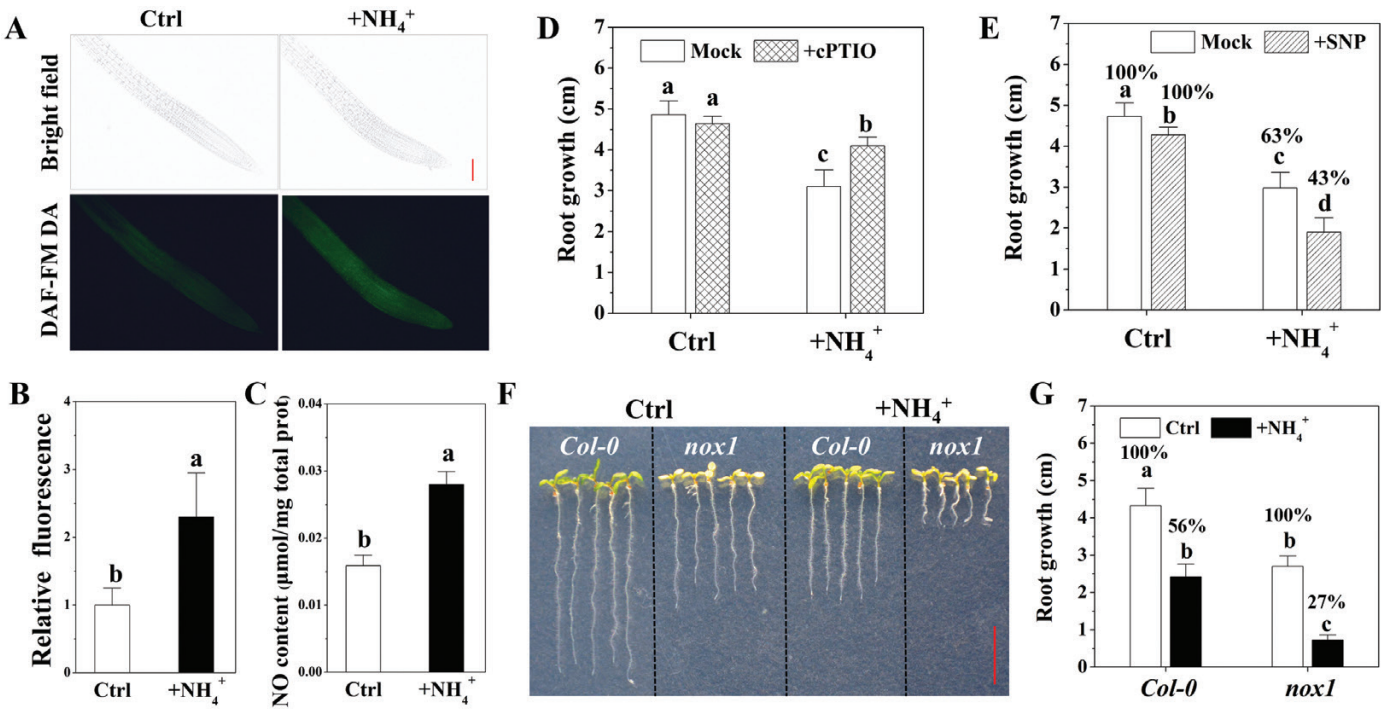

Fig. 1. Effect of nitric oxide (NO) on primary root growth under NH_4^+ in Arabidopsis. (A) The endogenous NO level in the primary root was monitored by labeling NO using the NO-specific fluorescent probe DAF-FM DA in 7-day-old seedlings grown on control (Ctrl) medium and in medium containing 10 mM NH_4^+ ($+NH_4^+$), imaged by epifluorescence microscopy. Scale bar=100 μm. (B) The mean relative DAF-FM fluorescence intensity in the primary root of 7-day-old control and NH_4^+-treated seedlings. The fluorescence intensity of the control was set to 1. Values shown are the means ±SD (n=5). (C) NO content in 7-day-old control and NH_4^+-treated seedlings. Values shown are the means ±SD of five replicates. The comparisons were carried out using an independent samples t-test (P<0.05). (D and E) Effect of the NO scavenger cPTIO (100 μM) and the NO donor SNP (1 μM) on primary root growth of Col-0 seedlings grown in control (Ctrl) and 10 mM NH_4^+ ($+NH_4^+$) medium. Values shown are the means ±SD (n=17–21). The percentage indicates the comparison between Ctrl and $+NH_4^+$ for the same treatment. Different letters represent means that are statistically different at the 0.05 level (one-way ANOVA with Duncan post-hoc test). (F and G) Effect of NH_4^+ on primary root growth in 7-day-old Col-0 and the NO-overproducting mutant *nox1* seedlings. Scale bar=1 cm. Values shown are the means ±SD (n≥17). The percentage indicates the comparison between Ctrl and $+NH_4^+$ in the same ecotype. Different letters represent means that are statistically different at the 0.05 level (one-way ANOVA with Duncan post-hoc test).

NO contributes to ammonium-inhibited K^+ homeostasis

To investigate whether NH_4^+ sensitivity of the *nox1* mutant is associated with increased tissue accumulation of NH_4^+, the NH_4^+ content was determined. NH_4^+ content was not found to be different between *nox1* and Col-0 under control and NH_4^+ treatments (Fig. 2A). Auxin transport and K^+ homeostasis had been suggested to be involved in NO-regulated root growth (Fernández-Marcos *et al.*, 2011; Simontacchi *et al.*, 2015; Zhang *et al.*, 2018); however, previous reports suggested that NH_4^+-inhibited root growth is largely independent of auxin transport (Li *et al.*, 2010; Liu *et al.*, 2013). A reduction in tissue K^+ has been frequently reported in connection with NH_4^+ toxicity. To assess whether endogenous NO levels in NH_4^+-treated plants are related to K^+ homeostasis, the K^+ content was first analyzed in Col-0 and NO-overproducing *nox1* seedlings. The K^+ content of *nox1* under control conditions was found to be significantly lower than that of Col-0 (Fig. 2B). When NH_4^+ was supplied, K^+ content in both Col-0 and *nox1* plants decreased, but the K^+ content of *nox1* was significantly lower than that of Col-0 (Fig. 2B). In agreement with genetic studies, treatment with the NO donor SNP significantly reduced K^+ content in Col-0 under both control and NH_4^+ treatment (Supplementary Fig. S1A). To further evaluate the role of NO in root K^+ accumulation under high NH_4^+, we measured net K^+ fluxes in root epidermal cells using NMT. NH_4^+ treatment reduced net K^+ influx in both Col-0 and *nox1*; however, K^+ influx was significant lower in *nox1* than in Col-0 under both control and NH_4^+ treatments (Fig. 2G), consistent with K^+ content analysis. The negative correlation between NO and K^+ content clearly suggests that NO contributes to NH_4^+-inhibited K^+ absorption in Arabidopsis.

The *SNO1/SOS4* gene encoding a pyridoxal kinase has been identified recently to play a critical role in NO-mediated root K^+ homeostasis, and the activity is induced by NO (Shi *et al.*, 2002; Xia *et al.*, 2014; Zhang *et al.*, 2018). Consistently, an increase in *SNO1/SOS4* activity was observed in NH_4^+-treated Col-0 and *nox1* seedlings; however, the induction was more significant in *nox1* (Fig. 2C). Compared with Col-0 controls, the *sno1/sos4* mutant exhibited enhanced root growth inhibition and significantly lower K^+ content and K^+ influx in response to NH_4^+ (Fig. 2D–G). NO and SNO1

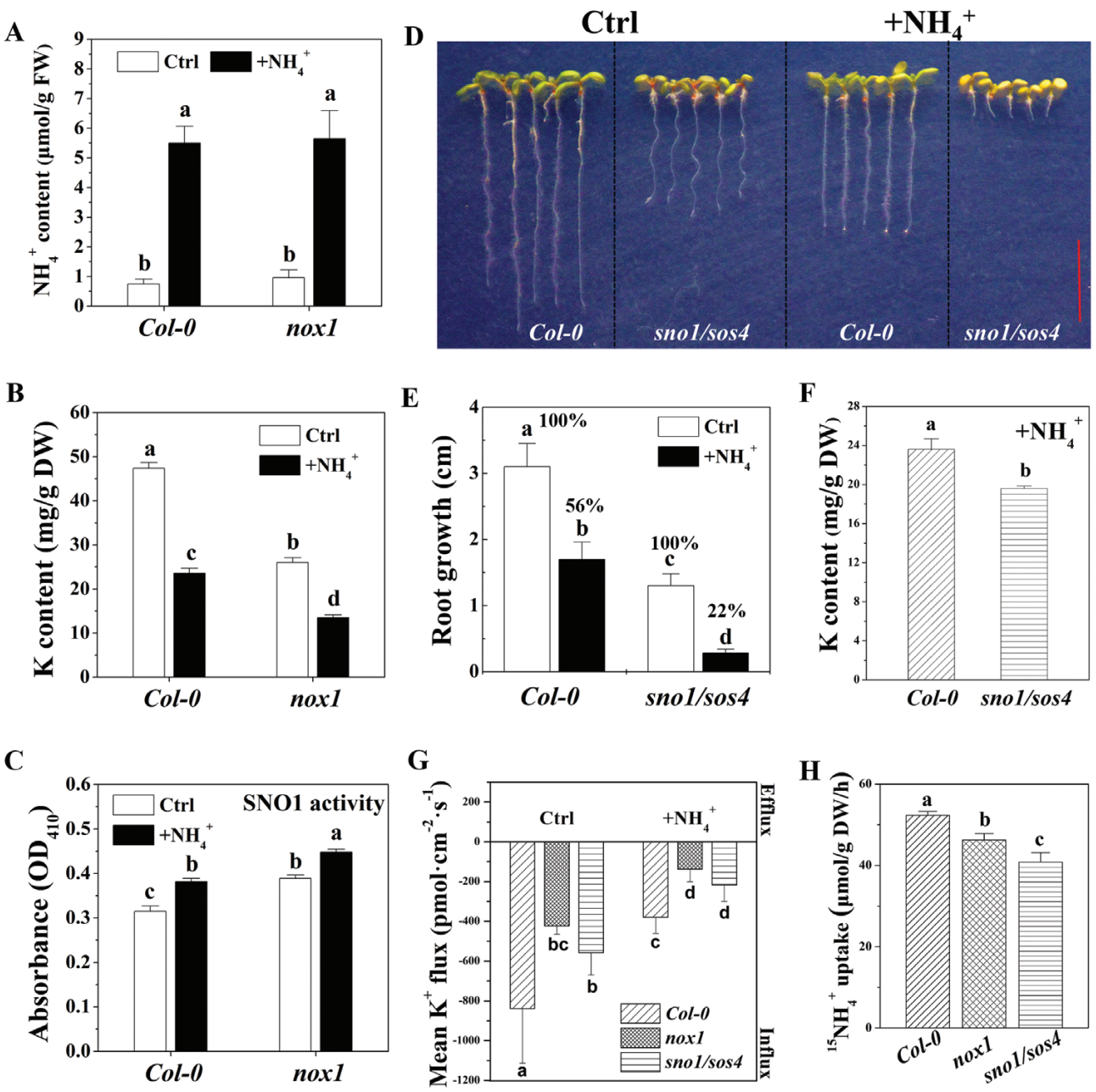

Fig. 2. Effects of NO on K^+ homeostasis under NH_4^+. (A) The NH_4^+ content in 7-day-old Col-0 and NO-overproducting mutant *nox1* seedlings. Values shown are the means ±SD of three replicates. (B) Effect of NH_4^+ (+NH_4^+, 10 mM) on K^+ content in 7-day-old wild-type (Col-0) and NO-overproducing mutant *nox1* seedlings. Values shown are the means ±SD of three replicates. (C) Enzyme activity of SNO1/SOS4 in 7-day-old Col-0 and NO-overproducting mutant *nox1* seedlings in response to NH_4^+ (10 mM). Values shown are the means ±SD of three replicates. (D and E) Effect of NH_4^+ on primary root growth in Col-0 and the *sno1/sos4* mutant. Scale bar=1 cm. Values shown are the means ±SD ($n \geq 18$). The percentage indicates the comparison between Ctrl and +NH_4^+ in the same ecotype. (F) Effect of NH_4^+ (+NH_4^+, 10 mM) on K^+ content in 7-day-old Col-0 and *sno1/sos4* seedlings. Values shown are the means ±SD of three replicates, and the comparisons were carried out using an independent samples *t*-test ($P<0.05$). (G) Net K^+ fluxes of Col-0, *nox1*, and *sno1/sos4* at the root mature zone. Values are the means ±SD, and more than five independent seedlings were analyzed in flux experiments. (H) $^{15}NH_4^+$ uptake of Col-0, *nox1*, and *sno1/sos4* seedlings. Values shown are the means ±SD of three replicates. Different letters represent means that are statistically different at the 0.05 level (one-way ANOVA with Duncan post-hoc test).

inhibit plant K^+ content via decreases in K^+ absorption, by inhibiting K^+ channels (Xia *et al.*, 2014). Consistently, addition of TEA, a well-known inhibitor of K^+ channel activity (Coskun *et al.*, 2010), generally led to a substantial reduction in root growth under NH_4^+ (Supplementary Fig. S1B). These results suggest that NO contributes to NH_4^+-inhibited K^+ absorption in Arabidopsis at least partly via enhanced SNO1/SOS4 activity.

The competition of NH_4^+ and K^+ at the site of K^+ transporters plays a role in inhibition of K^+ uptake by NH_4^+ (Szczerba *et al.*, 2008a, b; Balkos *et al.*, 2010; ten Hoopen *et al.*, 2010). To test whether NO-mediated lowering of K^+ uptake was linked to higher NH_4^+ absorption, we then compared the rate of NH_4^+ uptake by the roots of Col-0 plants with *nox1* and *sno1/sos4* mutants in a 10 mM $^{15}NH_4^+$ medium. However, root NH_4^+ uptake by *nox1* and *sno1/sos4* was lower than that of Col-0 (Fig. 2H), suggesting that lower K^+ absorption in *nox1* and *sno1/sos4* was not the result of higher NH_4^+ uptake.

GSNOR negatively regulates ammonium-mediated NO accumulation and K^+ imbalance

As NR is the key enzyme responsible for NO biosynthesis in plants, we first measured the effects of NH_4^+ on the expression of the NR-encoding genes NIA1 and NIA2 and the activity of NR. As shown in Fig. 3A and B and Supplementary Fig. S9B, NR-encoding gene expression and NR activity in Col-0 roots were not affected at all NH_4^+ concentrations tested compared with the control, consistent with a previous report (Engelsberger and Schulze, 2012). We further investigated the role of NR in NH_4^+-modulated root growth with the NR mutant *nia1nia2*. We found that the *nia1nia2* mutant exhibited a similar reduction in primary root growth to Col-0 (Fig. 3C). Furthermore, NOS activity was also tested and found not to be induced by NH_4^+ (Supplementary Fig. S2A). Similarly, infiltration with either L-NAME or L-NMME (inhibitors of animal NOS, also effective in plant systems) did not significantly modify NH_4^+ inhibition of primary root growth (Supplementary Fig. S2B), whereas these compounds have been shown to reduce the inhibitory effect of salt and Cd treatments on root growth (Liu *et al.*, 2015; Yuan and Huang, 2016). Furthermore, we tested the *noa1* (nitric oxide-associated protein 1) mutant, in which regulation of NO accumulation is suppressed via an unknown mechanism (Crawford *et al.*, 2006). As shown in Fig. 3C, the decrease in root length in *noa1* upon NH_4^+ exposure was also comparable with that in Col-0. These data suggest that the NH_4^+-mediated increase in NO and decrease in primary root length depend neither on NOA1 nor on NR and NOS.

Arabidopsis GSNOR is a master regulator of the intracellular NO level (see review in Li *et al.*, 2021). To determine whether GSNOR is involved in NH_4^+-mediated NO level changes, we first examined the expression of GSNOR. As shown in Fig. 3D and Supplementary Fig. S10A, NH_4^+ can induce root GSNOR expression, but the induction was independent of the NH_4^+ concentrations tested.

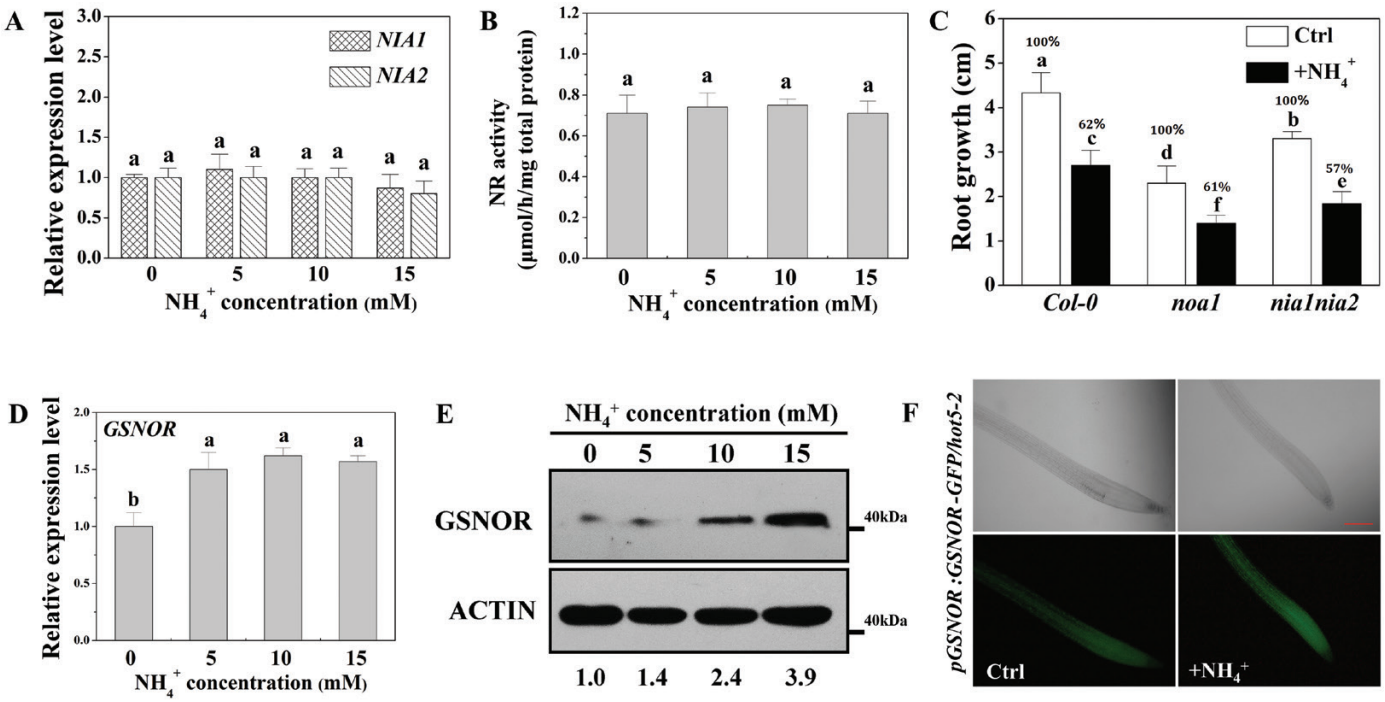

Fig. 3. Effect of NH_4^+ on nitrate reductase (NR) and GSNOR levels. (A) Effect of NH_4^+ on gene expression of NIA1 and NIA2 in 7-day-old Col-0 roots. Values shown are the means ±SD of three replicates. (B) Effect of NH_4^+ on NR activity in 7-day-old Col-0 roots. Values shown are the means ±SD of three replicates. (C) Effect of NH_4^+ (+NH_4^+, 10 mM) on primary roots of Col-0, *noa1*, and *nia1nia2*. Values shown are the means ±SD ($n \geq 17$). The percentage indicates the comparison between Ctrl and +NH_4^+ in the same ecotype. (D) GSNOR expression in the roots of 7-day-old Col-0 plants treated with varying concentrations of NH_4^+. Values shown are the means ±SD of three replicates. (E) Immunoblotting analysis of GSNOR in 7-day-old Col-0 seedling roots treated with varying concentrations of NH_4^+. The relative level of GSNOR protein was normalized to the actin level, as indicated at the bottom of the blots. (F) Fluorescence signal of root expressing *pGSNOR:GSNOR-GFP* at day 7 under control and 10 mM NH_4^+ (+NH_4^+) conditions. Scale bar=100 μm. Different letters represent means that are statistically different at the 0.05 level (one-way ANOVA with Duncan post-hoc test).

We further investigated GSNOR protein levels and found that the accumulation of GSNOR was also up-regulated by NH_4^+ in roots (Fig. 3E). The increase in GSNOR protein levels was further ascertained by complementation of *pGSNOR:GSNOR-GFP/hot5-2* transgenic plants in the *hot5-2/gsnor* mutant background (Xu *et al.*, 2013; Li *et al.*, 2019); GSNOR–GFP expression under NH_4^+ was higher than under control conditions (Fig. 3F). These results suggest that the accumulation of GSNOR protein is enhanced by NH_4^+.

Loss-of-function mutations in GSNOR have been reported to result in increased NO levels (Lee *et al.*, 2008; Chen *et al.*, 2009). Consistent with this, *hot5-2/gsnor* exhibited more NO accumulation relative to Col-0 under NH_4^+ (Fig. 4A). We further investigated the possible role of GSNOR in NH_4^+ inhibition of primary root growth. Exposure of *hot5-2/gsnor* to NH_4^+ led to more inhibition of root growth than in Col-0, with elongation being reduced by ~35% and ~62% in Col-0 and *hot5-2/gsnor*, respectively, upon exposure to NH_4^+ (Fig. 4B, C). Furthermore, the complementation line *pGSNOR:GSNOR-GFP/hot5-2* had similar root growth and NO content compared with Col-0 under NH_4^+ (Fig. 4D, E), confirming that the higher NO level and NH_4^+ sensitivity in *hot5-2/gsnor* was due to GSNOR loss of function. Next, we overexpressed GSNOR in Col-0 plants to study gene function. The high expression line (#1) exhibited slightly lower NH_4^+ inhibition compared with Col-0 and the low expression line (#2) (Supplementary Fig. S3). These results suggest that GSNOR positively regulates root growth tolerance to NH_4^+. The above data indicate that NO suppresses K^+ content under NH_4^+, while increasing SNO1/SOS4 activity. K^+ content and SNO1/SOS4 activity were further analyzed in Col-0 and *hot5-2/gsnor* plants treated with NH_4^+. Compared with Col-0, *hot5-2/gsnor* exhibited significantly lower K^+ content under NH_4^+ conditions (Fig. 4F). Moreover, higher *SNO1/SOS4* activity was observed in NH_4^+-treated *hot5-2/gsnor* (Fig. 4G). Consistent with this, *hot5-2/gsnor* had lower net K^+ influx under NH_4^+ conditions, compared with Col-0 (Fig. 4H). In the NH_4^+ medium, the rate of root $^{15}NH_4^+$ uptake by *hot5-2/gsnor* was also lower than in Col-0 (Fig. 6D), similar to *nox1* and *sno1/sos4*. These observations demonstrate that GSNOR negatively regulates the NO level and contributes to K^+ homeostasis and NH_4^+ tolerance of root growth.

Involvement of VTC1 in ammonium-regulated NO and GSNOR levels

The accumulation of GSNOR can be reduced by NO and the NO donor SNP (Chen *et al.*, 2009; Zhan *et al.*, 2018; Supplementary Fig. S4). Interestingly, NH_4^+ increased both NO and GSNOR levels in our current study. We further explored GSNOR accumulation in response to NH_4^+. Salt stress has been reported to significantly induce calmodulin 1 (*CaM1*) and *CaM4* gene expression and to inhibit GSNOR in Arabidopsis (Zhou *et al.*, 2016). However, various concentrations of NH_4^+ did not affect *CaM1* and *CaM4* gene expression (Supplementary Figs S5, S10B, C).

To further explore the components of the GSNOR pathway under NH_4^+ in Arabidopsis, we conducted IP-MS analysis in GSNOR–GFP transgenic Arabidopsis plants. We identified potential GSNOR-interacting proteins using this strategy (Supplementary Table S2). We first focused on proteins that were reported and predicted to be involved in NH_4^+ tolerance. Among the pull-down proteins identified, VTC1 (At2g39770) satisfied the criteria. It has been reported that a mutation in the *VTC1* gene confers hypersensitivity to NH_4^+ in terms of primary root growth (Qin *et al.*, 2008; Barth *et al.*, 2010). Under our experimental conditions, growth of the *vtc1-1* primary root was indeed more sensitive to NH_4^+ than that of Col-0 (Fig. 5A, B). We further asked whether VTC1 affects the GSNOR level. GSNOR gene expression was first analyzed in the roots of Col-0 and *vtc1-1* seedlings treated with or without NH_4^+. A similar induction level of the GSNOR gene was found in NH_4^+-treated roots in both Col-0 and *vtc1-1* (Fig. 5C; Supplemntary Fig. S10A). However, immunoblotting showed that GSNOR accumulation was reduced by NH_4^+ in *vtc1-1* (Fig. 5D). We found that GSNOR accumulation was up-regulated by NH_4^+ in Col-0 roots; conversely, when treated with NH_4^+, GSNOR was reduced in *vtc1-1* (Fig. 5D). These results suggest that VTC1 is involved in regulating GSNOR protein accumulation but does not greatly influence its gene transcript in response to NH_4^+.

Given that GSNOR negatively regulates NO accumulation under NH_4^+ (cf. Fig. 4), and VTC1 regulates GSNOR under NH_4^+, we further examined NO levels in *vtc1-1*. Compared with the control, exposure to NH_4^+ led to increased NO accumulation in *vtc1-1* compared with Col-0 (Fig. 6A, B). We also tested the effect of SNP under NH_4^+ on root growth. SNP significantly enhanced Col-0 root growth inhibition under NH_4^+, whereas it had no significant effect on the already short roots in *vtc1-1* (Supplementary Fig. S6). Taken together, these results demonstrate a high endogenous NO content in *vtc1-1* compared with Col-0 under NH_4^+. Similar to the *nox1* and *hot5-2/gsnor* mutants, the *vtc1-1* mutant exhibited lower K^+ content relative to Col-0 under NH_4^+ (Fig. 6C). However, the rate of root NH_4^+ uptake by *vtc1-1* plants was also lower than that of Col-0 (Fig. 6D).

We further asked whether enhanced endogenous NO levels in NH_4^+-treated *vtc1-1* plants are related to higher NR or NOS activity. As shown in Supplementary Fig. S7, the NOS activity in *vtc1-1* did not differ significantly from that in Col-0 under NH_4^+; meanwhile, *vtc1-1* exhibited slightly lower NR activity relative to Col-0. Moreover, *CaM1* and *CaM4* gene expression in *vtc1-1* did not differ significantly from that in Col-0 under various NH_4^+ conditions (Supplementary Fig. S5).

We next determined whether, and, if so, how VTC1 is modulated by NH_4^+. We first checked the levels of VTC1 mRNA and found no obvious change under various NH_4^+ concentrations

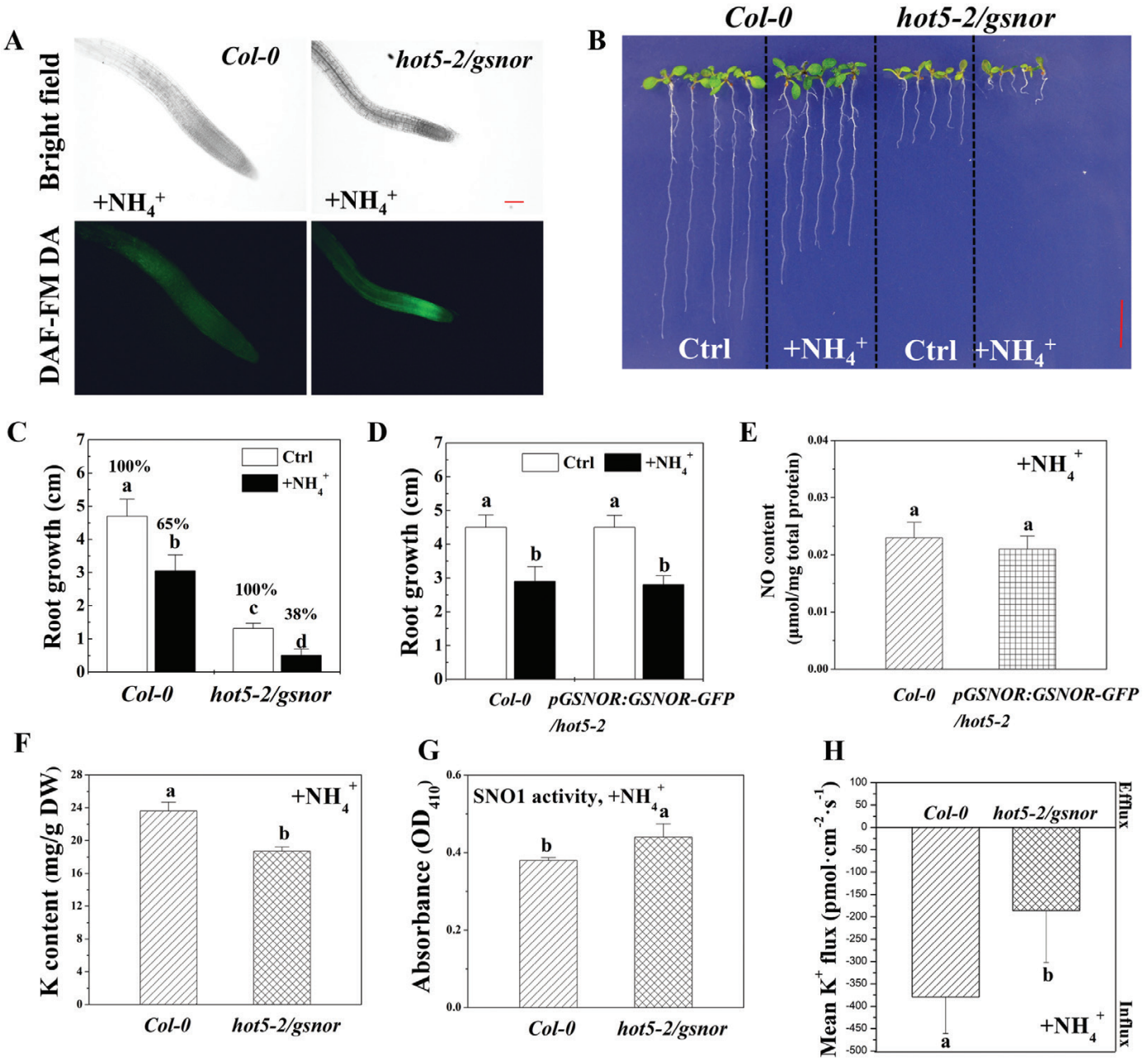

Fig. 4. Effect of loss of function of GSNOR on NH_4^+ sensitivity. (A) The endogenous NO level in the primary root was monitored by labeling NO using the NO-specific fluorescent probe DAF-FM DA of 7-day-old Col-0 and *hot5-2/gsnor* seedlings grown on 10 mM NH_4^+ ($+NH_4^+$) and imaged by epifluorescence microscopy. Scale bar=100 μm. (B and C) Effect of NH_4^+ on primary root growth in Col-0 and the *hot5-2/gsnor* mutant. Scale bar=1 cm. Values shown are the means ±SD (n=18). The percentage indicates the comparison between Ctrl and $+NH_4^+$ in the same ecotype. Different letters represent means that are statistically different at the 0.05 level (one-way ANOVA with Duncan post-hoc test). (D) Effect of NH_4^+ on primary root growth of Col-0 and *pGSNOR:GSNOR-GFP/hot5-2* transgenic plants. Values shown are the means ±SD (n=16–17). (E) NO content in Col-0 and *pGSNOR:GSNOR-GFP/hot5-2* transgenic plants under 10 mM NH_4^+ ($+NH_4^+$). Values shown are the means ±SD of five replicates. The comparisons were carried out using an independent samples t-test (P<0.05). (F) Effect of NH_4^+ ($+NH_4^+$, 10 mM) on K^+ content in 7-day-old Col-0 and *hot5-2/gsnor* seedlings. Values shown are the means ±SD of three replicates, and the comparisons were carried out using an independent samples t-test (P<0.05). (G) Enzyme activity of SNO1/SOS4 in 7-day-old Col-0 and *hot5-2/gsnor* seedlings under NH_4^+ ($+NH_4^+$, 10 mM). Values shown are the means ±SD of three replicates, and the comparisons were carried out using an independent samples t-test (P<0.05). (H) Mean values of net K^+ fluxes of Col-0 and *hot5-2/gsnor* at the root mature zone. Values are the means ±SD; >7 independent seedlings were analyzed in flux experiments and the comparisons were carried out using an independent samples t-test (P<0.05).

(Fig. 6E; Supplementary Fig. S9A). We further monitored the level of endogenous VTC1 protein, using an anti-VTC1-HA antibody, in response to various NH_4^+ concentrations. We found that the levels of VTC1 protein dramatically accumulated after NH_4^+ treatment (Fig. 6F), suggesting that NH_4^+ regulates VTC1 accumulation at the protein level.

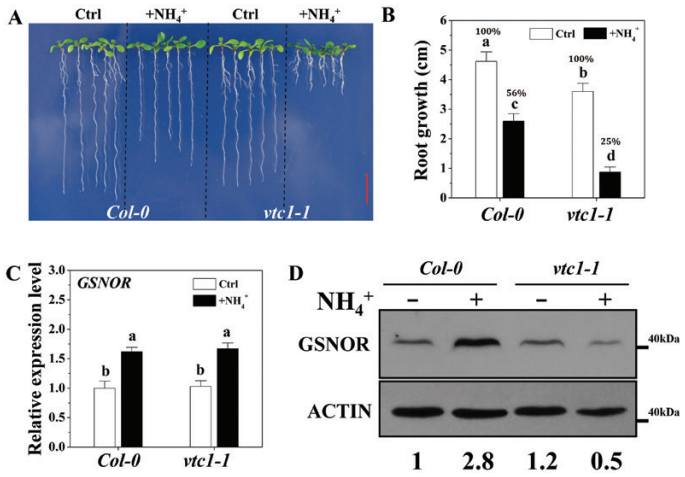

Fig. 5. Effect of loss of function of VTC1 on primary root growth and GSNOR level under NH_4^+. (A and B) Effect of NH_4^+ on primary root growth in Col-0 and the *vtc1-1* mutant. Scale bar=1 cm. Values shown are the means ±SD ($n \geq 14$). The percentage indicates the comparison between Ctrl and $+NH_4^+$ in the same ecotype. (C) Effect of NH_4^+ (10 mM) on GSNOR expression of 7-day-old Col-0 and *vtc1-1* seedling roots. Values shown are the means ±SD of three replicates. (D) Immunoblotting analysis of GSNOR in 7-day-old Col-0 and *vtc1-1* seedling roots treated with (+) or without (–) 10 mM NH_4^+. The relative level of GSNOR protein was normalized with the actin level, as indicated at the bottom of the blots. Different letters represent means that are statistically different at the 0.05 level (one-way ANOVA with Duncan post-hoc test).

GSNOR overexpression enhances vtc1-1 *mutant tolerance to ammonium*

Because VTC1 can regulate GSNOR under NH_4^+, we next generated transgenic *GSNOR-OX/vtc1-1* overexpression lines (Fig. 7A), to examine the genetic interaction between VTC1 and GSNOR in Arabidopsis. Intriguingly, compared with *vtc1-1*, GSNOR overexpression in the *vtc1-1* background presented relatively greater primary root growth under NH_4^+ (Fig. 7B, C). Next, we examined NO levels in the *GSNOR-OX/vtc1-1* transgenic lines, and overexpression of GSNOR in *vtc1-1* led to lower NO levels than in the *vtc1-1* mutant under NH_4^+ (Fig. 7D, E). These results indicate that GSNOR functions downstream of VTC1 to regulate NO and primary root growth in response to NH_4^+.

OsGSNOR is required for ammonium tolerance in rice

The critical function of GSNOR in conferring tolerance to NH_4^+ in Arabidopsis prompted us to test whether it is conserved in rice, which typically grows in NH_4^+-rich soils (Kronzucker *et al.*, 2000). GSNOR exists as a single copy of the genome in most plant species, including rice (Li *et al.*, 2019; Fig. 8A). We chose a knockout of OsGSNOR (Os02G57040), using the CRISPR/Cas9 system, to test the contribution of OsGSNOR in the NH_4^+ tolerance of rice. Similar to Arabidopsis, the root growth in two OsGSNOR knockout lines (*Osgsnor-1* and *Osgsnor-2*) was also significantly more sensitive to NH_4^+ than in the wild type (Fig. 8B–D). Moreover, compared with the wild type, the root K^+ content in *Osgsnor* knockout lines was also lower under NH_4^+ (Fig. 8E). Thus, the OsGSNOR also contributes to both K^+ homeostasis and root growth tolerance to NH_4^+ in rice.

Discussion

NH_4^+ toxicity is well known to inhibit primary root growth (Britto and Kronzucker, 2002; Li *et al.*, 2014), yet our understanding of the mechanism behind this has remained limited. Herein, we present an important link between the previously identified player VTC1 (Qin *et al.*, 2008; Barth *et al.*, 2010) and GSNOR in protecting primary root growth under NH_4^+ toxicity. VTC1 and GSNOR are shown to support root tolerance to NH_4^+ by negatively regulating NO accumulation and by protecting K^+ homeostasis.

In contrast to the studies on the role of NO in plant responses to other nutrient stresses (e.g. Cu and Al; Tian *et al.*, 2007; Peto *et al.*, 2013), the role of NO in the regulation of root growth under NH_4^+ challenge has not been hitherto investigated. Here, we demonstrate that root growth effects under NH_4^+ in Arabidopsis are mediated, at least in part, by NO accumulation, and we show this by using both pharmacological and genetic approaches. A positive, root-growth-protective, role of NO has been found under Cu and Al toxicity and under conditions of P and Fe deficiency in Arabidopsis (Tian *et al.*, 2007; Chen *et al.*, 2010; Peto *et al.*, 2013; Royo *et al.*, 2015). These differences may be explained by the fact that NO can cause opposite effects in cells depending on its cellular localization and intracellular concentration (Leitner *et al.*, 2009; Gill *et al.*, 2013; Yuan and Huang, 2016). Alternatively, NO production from different sources may also lead to divergent effects (Xiong *et al.*, 2010; Zhang *et al.*, 2018), even in the context of the same stress response. It has been demonstrated that NR and/or NOS are involved in NO generation under Cu excess and Al toxicity, and P deficiency and Fe deficiency in Arabidopsis roots (Tian *et al.*, 2007; Chen *et al.*, 2010; Peto *et al.*, 2013; Sun *et al.*, 2014; Royo *et al.*, 2015). NOS has also been reported to be involved in salt stress-mediated NO production (Liu *et al.*, 2015), resulting in enhanced salt tolerance of Arabidopsis root growth (Zhao *et al.*, 2007; Zhou *et al.*, 2016). In contrast, previous and present results found that NH_4^+ toxicity did not affect the expression of the Arabidopsis NR-coding gene *NIA2* (Hachiya *et al.*, 2012; Fig. 3A). Our present data furthermore show that NH_4^+ does not affect NR and NOS activity in Arabidopsis roots, and the NOS inhibitors L-NAME and L-NMME and mutations in NOA1, NIA1, and NIA2 have no significant effect on NH_4^+-inhibited root growth (Fig. 3; Supplementary Fig. S2). At least seven possible pathways for NO biosynthesis have been described in plants (Gupta *et al.*, 2011; Yu *et al.*, 2014). However, to date, the identity of the NO biosynthesis pathway engaged under NH_4^+ toxicity in plants has remained unidentified.

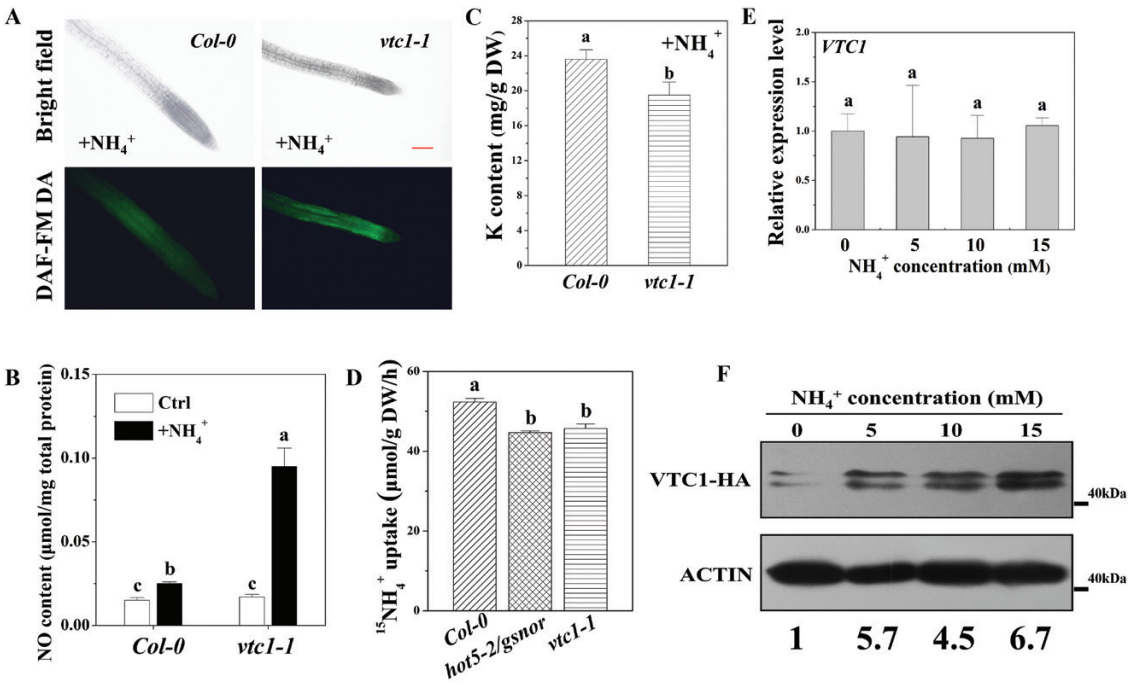

Fig. 6. Effect of loss of function of VTC1 on NO accumulation and K^+ level under NH_4^+. (A) The endogenous NO level in the primary root of 7-day-old Col-0 and *vtc1-1* seedlings grown on 10 mM NH_4^+ ($+NH_4^+$), monitored by labeling NO using the NO-specific fluorescent probe DAF-FM DA, imaged by epifluorescence microscopy. Scale bar=100 μm. (B) NO content in 7-day-old control and NH_4^+-treated Col-0 and *vtc1-1* seedlings. Values shown are the means ±SD of five replicates. (C) Effect of NH_4^+ ($+NH_4^+$, 10 mM) on K^+ content in 7-day-old Col-0 and *vtc1-1* seedlings. Values shown are the means ±SD of three replicates, and the comparisons were carried out using an independent samples *t*-test ($P<0.05$). (D) $^{15}NH_4^+$ uptake of Col-0, *hot5-2/gsnor*, and *vtc1-1* seedlings. Values shown are the means ±SD of three replicates. (E) Effect of NH_4^+ on VTC1 gene expression. VTC1 expression in the roots of 7-day-old Col-0 plants treated with varying concentrations of NH_4^+. Values shown are the means ±SD of three replicates. (F) Immunoblotting analysis of VTC1-HA in 7-day-old Col-0 seedling roots treated with varying concentrations of NH_4^+. The relative level of VTC1-HA protein was normalized with the actin level, as indicated at the bottom of the blots. Different letters represent means that are statistically different at the 0.05 level (one-way ANOVA with Duncan post-hoc test).

Although it is not known how NH_4^+ induces NO biosynthesis at present, once NO is formed, there must be mechanisms to decrease its concentration. GSNOR is an important and widely utilized component of resistance protein signaling networks that control NO accumulation (Zhou *et al.*, 2016; Zhang *et al.*, 2020). In this study, the loss of GSNOR function resulted in a higher NO level and enhanced NH_4^+ sensitivity compared with wild-type plants, implying that GSNOR is a positive regulator of NH_4^+ tolerance by inhibiting NO accumulation. Furthermore, NH_4^+ enhanced GSNOR transcription and protein levels. GSNOR protein accumulation may be independent of CaM1 and CaM4 functions, as the expression of *CaM1* and *CaM4* genes was not responsive to NH_4^+ and, more importantly, did not affect GSNOR protein levels (Zhou *et al.*, 2016). Here, using IP-MS assays for analyzing GSNOR–GFP plants, precipitated VTC1 protein was identified (Supplementary Table S2). VTC1, which was the first NH_4^+-responsive gene identified through forward genetics, when mutated, confers significant NH_4^+ sensitivity on primary root growth, although the mechanisms underpinning this have remained obscure (Qin *et al.*, 2008; Li *et al.*, 2010; Kempinski *et al.*, 2011; Fig. 5A, B). We furthermore found that GSNOR protein accumulation under NH_4^+ was dependent on VTC1 gene function in Arabidopsis. Supporting this is the observation that NH_4^+ induced GSNOR accumulation in Col-0 but decreased it in the *vtc1-1* mutant, although GSNOR gene expression was not affected. In contrast, there was no difference in the GSNOR protein level in the absence of NH_4^+ (Fig. 5D), suggesting that the regulation of GSNOR involving VTC1 is NH_4^+ dependent. Barth *et al.* (2010) suggested that NH_4^+ hypersensitivity in *vtc1-1* may be associated with NO signaling. The present data confirm an NO-overaccumulation phenotype of *vtc1-1*. However, unlike in the previous study, we here show that NH_4^+-mediated NO production in *vtc1-1* does not occur via the NR and NOS enzyme pathways. Although a higher expression of the *NOA1* gene in the NH_4^+-treated *vtc1-1* mutant was found in a previous report (Barth *et al.*, 2010), the *NOA1* gene mutation had no effect on root growth under NH_4^+ (Fig. 3C). Furthermore, enhanced NOA1 expression was also reported to not increase plant NO levels (Kato *et al.*, 2008). GSNOR probably functions downstream of VTC1 in response to NH_4^+ (Fig. 7). Thus, in consideration of the roles of GSNOR in regulating NO accumulation, GSNOR may be an important factor conferring NH_4^+-mediated NO

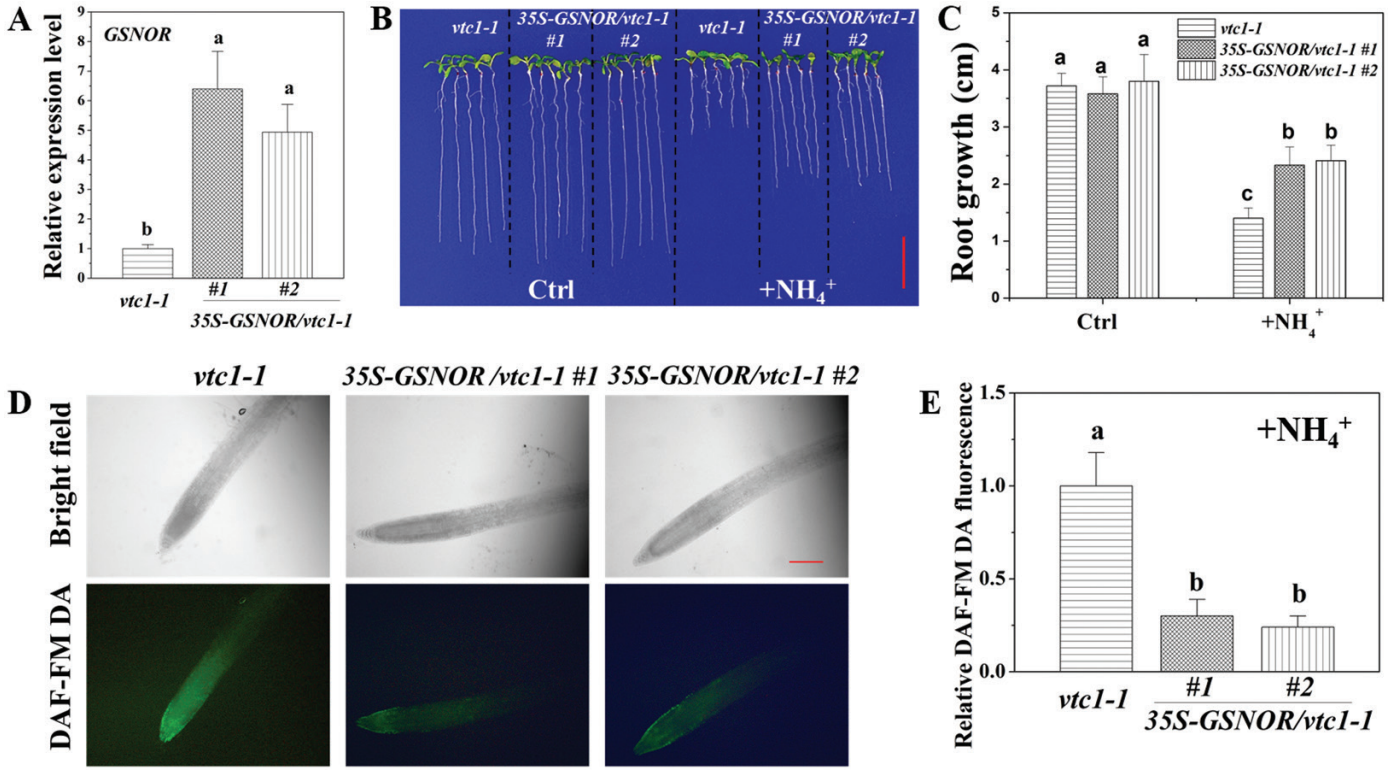

Fig. 7. Effect of GSNOR overexpression in the *vtc1-1* mutant on the primary root growth and NO level in response to NH_4^+. (A) *GSNOR* gene expression in *vtc1-1* and two overexpression lines (*35S-GSNOR/vtc1-1* #1 and #2). Values shown are the means ±SD of three replicates. (B and C) Effect of NH_4^+ on primary root growth in 7-day-old *vtc1-1* and GSNOR overexpression lines. Scale bar=1 cm. Values shown are the means ±SD ($n \geq 14$). Seedlings were grown in control (Ctrl) and 10 mM NH_4^+ (+NH_4^+) medium for 7 d. (D) The endogenous NO level in the primary root was monitored by labeling NO using the NO-specific fluorescent probe DAF-FM DA in 7-day-old seedlings grown on 10 mM NH_4^+ (+NH_4^+), imaged by epifluorescence microscopy. Scale bar=100 μm. (E) The mean relative DAF-FM fluorescence intensity in the primary root of NH_4^+-treated (+NH_4^+) seedlings. The fluorescence intensity of the *vtc1-1* mutant was set to 1. Values shown are the means ±SD (n=6–7). Different letters represent means that are statistically different at the 0.05 level (one-way ANOVA with Duncan post-hoc test).

overaccumulation in *vtc1-1*. In contrast, the disappearance of GSNOR enrichment in *vtc1-1* under NH_4^+ may further aggravate the accumulation of NO in this mutant. One possible explanation is that a VTC1-mediated glycosylation modification may be involved in protecting GSNOR protein stability under NH_4^+. VTC1 could catalyze the reversible synthesis of GDP-mannose, which is an important intermediate required for *N*-glycosylation of proteins (Qin *et al.*, 2008; Jadid *et al.*, 2011; Tanaka *et al.*, 2015). Defective *N*-glycosylation of proteins was observed in *vtc1* mutant roots grown in the presence of NH_4^+ (Qin *et al.*, 2008). Glycosylation can increase the stability of proteins under a variety of denaturation conditions and can prevent protein aggregation; meanwhile, the sugar chains on the protein surface can also cover some degradation sites by protease in protein molecules, thus increasing protein resistance to proteases (Helenius and Aebi, 2001; Jadid *et al.*, 2011). NO has been suggested to regulate Arabidopsis GSNOR stability by *S*-nitrosylation followed by GSNOR degradation through selective autophagy (Zhan *et al.*, 2018). Whether VTC1 can affect *S*-nitrosylation or selective autophagy is not clear at present. Alternatively, VTC1 may be involved in enhancing the NO level under NH_4^+, thus protecting GSNOR from *S*-nitrosylation. More research is warranted to examine the mechanisms of VTC1 in regulating GSNOR levels.

Maintaining a higher tissue K^+ level can effectively alleviate NH_4^+ toxicity (Szczerba *et al.*, 2006, 2008*b*; Balkos *et al.*, 2010). Many physiological studies have shown that lower uptake of cations, especially of K^+, is one of the key features of NH_4^+ toxicity (Li *et al.*, 2012; Bittsánszky *et al.*, 2015). NH_4^+ potently reduces K^+ uptake and content in plant roots (Szczerba *et al.*, 2008*b*; Li *et al.*, 2012), in part because of direct ion competition (ten Hoopen *et al.*, 2010), as NH_4^+ and K^+ have identical charges and similar hydrated radii. Coskun *et al.* (2013) found that increased external K^+ concentration can also reduce NH_3/NH_4^+ influx. There may be reciprocal inhibition between potassium and ammonium (Britto and Kronzucker, 2008; Coskun *et al.*, 2017a). Although the detailed mechanism behind this remains to be explored, identical charges and similar hydrated radii between the two ions are likely to play a role. No signals have thus far been identified that mediate the original NH_4^+ signal to regulate K^+ acquisition. In the present study, employing both pharmacological and genetic approaches, we

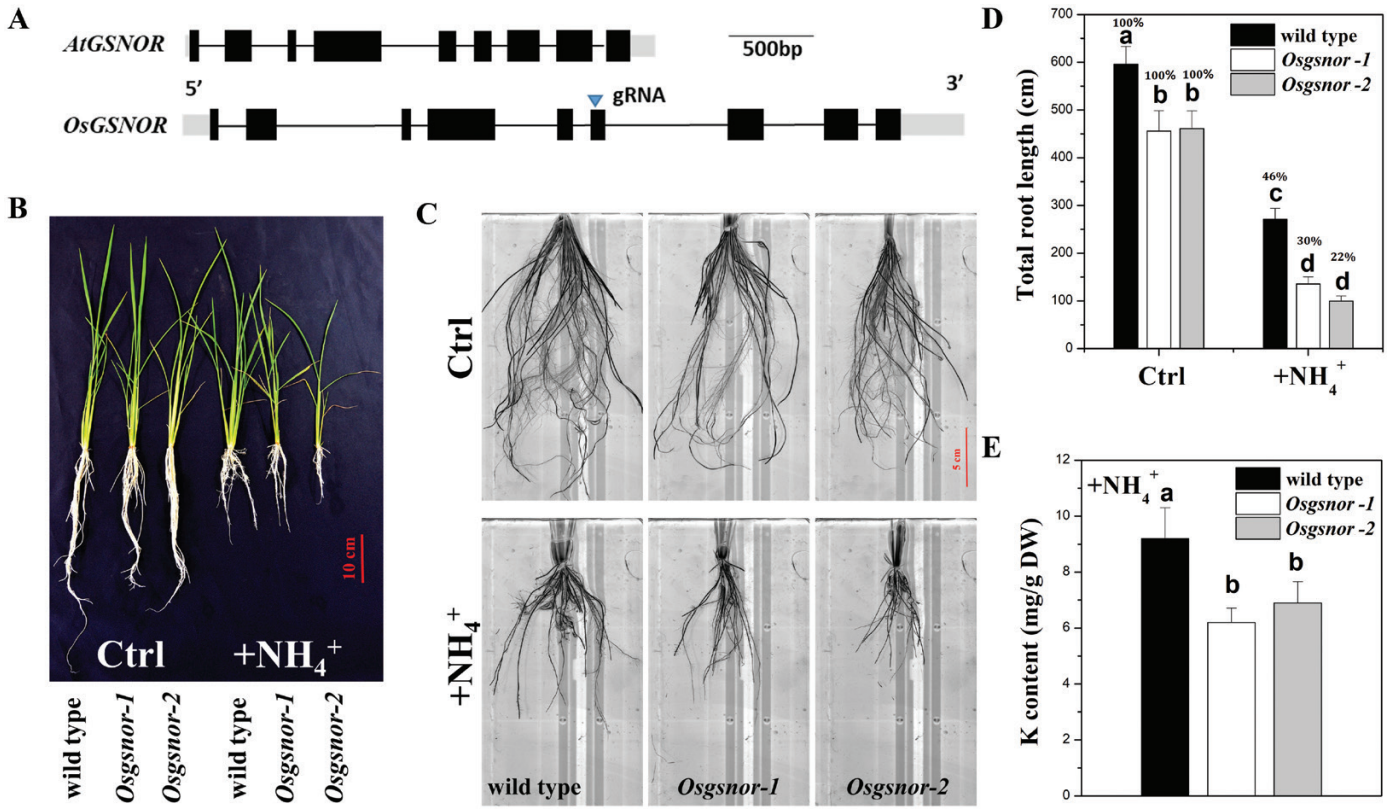

Fig. 8. Effect of loss of function of OsGSNOR on NH_4^+ sensitivity of roots in rice. (A) Schematic representation of the gene structures and alleles of GSNOR from Arabidopsis and rice. Blue triangles indicate the position of guide RNA (gRNA) for CRISPR/Cas9. (B) Growth of CRISPR/Cas9 knockout lines of OsGSNOR and the wild type under Ctrl and $+NH_4^+$ (10 mM) for 10 d. (C) Roots were dispersed in water for total root length analysis under Ctrl and $+NH_4^+$ for 10 d. (D) Quantified total root length is shown for OsGSNOR and the wild type under Ctrl and $+NH_4^+$ for 10 d. Values shown are the means ±SD (n=6). The percentage indicates the comparison between Ctrl and $+NH_4^+$ in the same ecotype. (E) Root K^+ content of CRISPR/Cas9 knockout lines in OsGSNOR and the wild type under NH_4^+ ($+NH_4^+$) for 10 d. Values shown are the means ±SD of three replicates. Different letters represent means that are statistically different at the 0.05 level (one-way ANOVA with Duncan post-hoc test).

show that an NH_4^+-induced rise in NO level is associated with the reduction in K^+ uptake, in turn disrupting K^+ homeostasis in Arabidopsis. We found that K^+ content and absorption in the NO-overproducting mutant *nox1*, and in *hot5-2/gsnor* and *vtc1-1*, which possess higher NO accumulation under NH_4^+, were significantly lower than those in Col-0 under NH_4^+. In support of this observation, supplying the NO donor SNP reduced tissue K^+ content more significantly than NH_4^+ alone. Moreover, the GSNOR-like gene, OsGSNOR, is also required for NH_4^+ tolerance and maintenance of K^+ content in rice in our study. Although the mechanism by which endogenous NO regulates K^+ absorption and homeostasis under NH_4^+ toxicity remains to be defined, one hypothesis is that NO influences K^+ channels. Recently, it has been reported that NO negatively regulates K^+ channel-mediated potassium uptake in roots through indirect modulation of SNO1/SOS4 in Arabidopsis (Xia *et al.*, 2014). Here, we provide evidence that an increase in SNO1/SOS4 activity occurs in NH_4^+-treated Col-0 and in NO-overaccumulatng mutants, and that this activity is additionally elevated in *nox1* and *hot5-2/gsnor* under NH_4^+ (Figs 2C, 6G). Accordingly, SNO1/SOS4 is also involved in the root growth response under NH_4^+ and in the regulation of K^+ content (Fig. 2D–F). Interestingly, NH_4^+ uptake in NO-overaccumulating mutants was lower than that of the wild type, suggesting that the lower K^+ absorption in these NO mutants is not the result of enhanced competition with the chemically similar NH_4^+ ion. All the data suggest that there is an NO-mediated inhibitory mechanism in addition to competition involved in the NH_4^+ inhibition of K^+ uptake. The lower NH_4^+ absorption in NO-overaccumulating mutants could be due to more inhibited cation channel activity more generally, as has been shown for K^+ channels, resulting in reduced NH_4^+ absorption via cation channels. Although it is not known at this time how NO and SNO1/SOS4 engage to modulate root K^+ uptake and homeostasis under NH_4^+, the present results provide important new insights for future studies on the interactions between NH_4^+ and K^+, and more detailed research is warranted to examine this in the future. It should be noted that application of the channel inhibitor TEA, well known to inhibit K^+ channels, can reduce NH_4^+ influx while also inhibiting K^+ uptake under NH_4^+ conditions (Balkos *et al.*, 2010; ten Hoopen *et al.*, 2010; Coskun *et al.*,

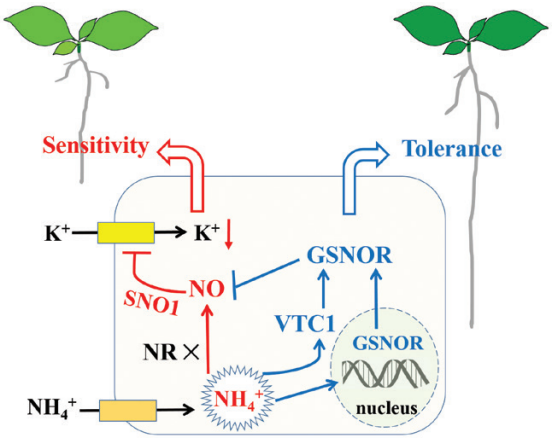

Fig. 9. A proposed model illustrating the role of GSNOR in plant NH_4^+ tolerance. Under high NH_4^+, NH_4^+ enters plant cells through K^+ channels by a competitive mechanism (ten Hoopen *et al.*, 2010), but also partly through other channels (Balkos *et al.*, 2010). NO levels and SNO1/SOS4 in roots are increased significantly and are involved in the arrest of K^+ uptake and primary root growth in an NH_4^+ environment. NO-linked lowering of K^+ absorption does not result from higher NH_4^+ uptake. NH_4^+-induced NO accumulation does not occur via the traditional NR (nitrate reductase) pathway. NH_4^+-induced GSNOR accumulation, as a compensator, can partially antagonize NO overaccumulation and protect root growth under NH_4^+ in the wild type. VTC1-linked GSNOR protein accumulation, but not gene expression, appears to be one key component of the signal transduction pathway under NH_4^+.

2013), contributing to Arabidopsis root growth inhibition under NH_4^+ toxicity (ten Hoopen *et al.*, 2010; Supplementary Fig. S1B). These results confirm that NH_4^+-inhibited K^+ accumulation aggravates NH_4^+ sensitivity.

In conclusion, we propose the following model for the role of GSNOR accumulation in plant NH_4^+ tolerance (Fig. 9): under high external NH_4^+ supply, NH_4^+ enters tissues through K^+ channels by competitive mechanisms (ten Hoopen *et al.*, 2010), and partly through other channels (Balkos *et al.*, 2010). NH_4^+-induced NO accumulation does not occur via traditional NR pathways. NO levels and SNO1/SOS4 in roots are increased significantly and are involved in the arrest of K^+ uptake and primary root growth under NH_4^+. Meanwhile, NH_4^+ induced GSNOR functions, as a compensator, to partially antagonize the induction of NO overaccumulation and protect root growth under NH_4^+ in the wild type. The exact mechanism by which NH_4^+ induces GSNOR remains to be resolved; however, VTC1-linked GSNOR protein regulation under NH_4^+ may be one component of the signal transduction pathway. Our results provide novel insight into how VTC1 and GSNOR interact to regulate NH_4^+ tolerance. GSNOR-regulated NH_4^+ tolerance was also found in rice, which is grown in soils where NH_4^+ is the predominant N form. Further research into the mechanisms of interplay between NH_4^+ and the NO signaling pathway in plants will enable a fuller understanding of how plants respond to varying extents of NH_4^+ stress, and will be instrumental in the development of strategies to improve NH_4^+ tolerance of crops.

Supplementary data

The following supplementary data are available at *JXB* online.

Fig. S1. Effect of SNP and TEA on NH_4^+ sensitivity.

Fig. S2. Effect of NH_4^+ on nitric oxide synthase (NOS) activity.

Fig. S3. Effect of GSNOR overexpression on Col-0 primary root growth.

Fig. S4. Effect of SNP on the GSNOR level.

Fig. S5. Effect of NH_4^+ on expression of *CaM1* and *CaM4* genes.

Fig. S6. Effect of SNP on primary root growth of Col-0 and *vtc1-1* seedlings under NH_4^+.

Fig. S7. Nitrate reductase (NR) and nitric oxide synthase (NOS) activities in Col-0 and *vtc1-1* under NH_4^+.

Fig. S8. Stable expression of the reference gene *ACTIN2* in different samples.

Fig. S9. *VTC1*, *NIA1*, and *NIA2* expression in Col-0 under varying NH_4^+ concentrations using the alternative reference gene *CBP20*.

Fig. S10. *GSNOR*, *CaM1*, and *CaM4* expression in Col-0 and *vtc1-1* under varying NH_4^+ concentrations using the alternative reference gene *CBP20*.

Table S1. The primers used in this study.

Table S2. List of proteins identified in immunoprecipitation-mass spectrometry of GSNOR–GFP.

Acknowledgements

We thank Dr Elizabeth Vierling (University of Massachusetts), Dr Xiaofang Zhu (Institute of Soil Science, Chinese Academy of Sciences), and Dr Rongfeng Huang (Biotechnology Research Institute, Chinese Academy of Agricultural Sciences) for providing the seeds of *proGSNOR:GSNOR-GFP/hot5-2*, *hot5-2/gsnor*, *nia1nia2*, and *35S:VTC1-HA*/Col-0, and the ABRC of Ohio State University for *nox1*, *noa1*, *vtc1*, and *sno1/sos4* mutant seeds. The work was supported by the National Key R&D Program of China (nos 2017YFD0200103 and 2017YFD0200100), the National Natural Science Foundation of China (no. 31972990), the Natural Science Foundation of Jiangsu Province (no. BK20200050), and the University of Melbourne.

Author contributions

LZ, HS, and GL: performing the experiments; GL, WS, BL, MW, and DW: conceptualization; LZ, HS, GL, BL, MW, and DW: data analysis; GL and WS: project administration, supervision; GL: writing—original draft; BL, YL, and HK: writing—review and editing; GL: funding acquisition.

Conflict of interest

The authors declare that they have no conflicts of interest.

Data availability

All data supporting the findings of this study are available within the paper and within its supplementary data published online.

References

Alemayehu A, Zelinová V, Bočová B, Huttová J, Mistrík I, Tamás L. 2015. Enhanced nitric oxide generation in root transition zone during the early stage of cadmium stress is required for maintaining root growth in barley. Plant and Soil **390**, 213–222.

Balkos KD, Britto DT, Kronzucker HJ. 2010. Optimization of ammonium acquisition and metabolism by potassium in rice (*Oryza sativa* L. cv. IR-72). Plant, Cell & Environment **33**, 23–34.

Barth C, Gouzd ZA, Steele HP, Imperio RM. 2010. A mutation in GDP-mannose pyrophosphorylase causes conditional hypersensitivity to ammonium, resulting in *Arabidopsis* root growth inhibition, altered ammonium metabolism, and hormone homeostasis. Journal of Experimental Botany **61**, 379–394.

Besson-Bard A, Pugin A, Wendehenne D. 2008. New insights into nitric oxide signaling in plants. Annual Review of Plant Biology **59**, 21–39.

Bittsánszky A, Pilinszky K, Gyulai G, Komives T. 2015. Overcoming ammonium toxicity. Plant Science **231**, 184–190.

Britto DT, Kronzucker HJ. 2002. NH_4^+ toxicity in higher plants: a critical review. Journal of Plant Physiology **159**, 567–584.

Britto DT, Kronzucker HJ. 2008. Cellular mechanisms of potassium transport in plants. Physiologia Plantarum **133**, 637–650.

Britto DT, Kronzucker HJ. 2013. Ecological significance and complexity of N-source preference in plants. Annals of Botany **112**, 957–963.

Britto DT, Szczerba MW, Kronzucker HJ. 2006. A new, non-perturbing, sampling procedure in tracer exchange measurements. Journal of Experimental Botany **57**, 1309–1314.

Chaki M, Valderrama R, Fernández-Ocaña AM, *et al.* 2010. Mechanical wounding induces a nitrosative stress by down-regulation of GSNO reductase and an increase in S-nitrosothiols in sunflower (*Helianthus annuus*) seedlings. Journal of Experimental Botany **62**, 1803–1813.

Chamizo-Ampudia A, Sanz-Luque E, Llamas A, Galvan A, Fernandez E. 2017. Nitrate reductase regulates plant nitric oxide homeostasis. Trends in Plant Science **22**, 163–174.

Chen R, Sun S, Wang C, *et al.* 2009. The *Arabidopsis PARAQUAT RESISTANT2* gene encodes an S-nitrosoglutathione reductase that is a key regulator of cell death. Cell Research **19**, 1377–1387.

Chen WW, Yang JL, Qin C, Jin CW, Mo JH, Ye T, Zheng SJ. 2010. Nitric oxide acts downstream of auxin to trigger root ferric-chelate reductase activity in response to iron deficiency in *Arabidopsis*. Plant Physiology **154**, 810–819.

Coskun D, Britto DT, Kronzucker HJ. 2010. Regulation and mechanism of potassium release from barley roots: an in planta $42K^+$ analysis. New Phytologist **188**, 1028–1038.

Coskun D, Britto DT, Kronzucker HJ. 2017*a*. The nitrogen–potassium intersection: membranes, metabolism, and mechanism. Plant, Cell & Environment **40**, 2029–2041.

Coskun D, Britto DT, Li M, Becker A, Kronzucker HJ. 2013. Rapid ammonia gas transport accounts for futile transmembrane cycling under NH_3/NH_4^+ toxicity in plant roots. Plant Physiology **163**, 1859–1867.

Coskun D, Britto DT, Shi W, Kronzucker HJ. 2017*b*. How plant root exudates shape the nitrogen cycle. Trends in Plant Science **22**, 661–673.

Coskun D, Britto DT, Shi W, Kronzucker HJ. 2017*c*. Nitrogen transformations in modern agriculture and the role of biological nitrification inhibition. Nature Plants **3**, 17074.

Crawford N, Galli M, Tischner R, Heimer Y, Okamoto M, Mack A. 2006. Response to Zemojtel *et al*: plant nitric oxide synthase: back to square one. Trends in Plant Science **11**, 526–527.

Crawford NM, Guo FQ. 2005. New insights into nitric oxide metabolism and regulatory functions. Trends in Plant Science **10**, 195–200.

Drescher GL, da Silva LS, Sarfaraz Q, Roberts TL, Nicoloso FT, Schwalbert R, Marques ACR. 2020. Available nitrogen in paddy soils depth: influence on rice root morphology and plant nutrition. Journal of Soil Science and Plant Nutrition **20**, 1029–1041.

Engelsberger WR, Schulze WX. 2012. Nitrate and ammonium lead to distinct global dynamic phosphorylation patterns when resupplied to nitrogen-starved *Arabidopsis* seedlings. The Plant Journal **69**, 978–995.

Fernández-Marcos M, Sanz L, Lewis DR, Muday GK, Lorenzo O. 2011. Nitric oxide causes root apical meristem defects and growth inhibition while reducing PIN-FORMED 1 (PIN1)-dependent acropetal auxin transport. Proceedings of the National Academy of Sciences, USA **108**, 18506–18511.

Frungillo L, Skelly MJ, Loake GJ, Spoel SH, Salgado I. 2014. S-nitrosothiols regulate nitric oxide production and storage in plants through the nitrogen assimilation pathway. Nature Communications **5**, 5401.

Gill SS, Hasanuzzaman M, Nahar K, Macovei A, Tuteja N. 2013. Importance of nitric oxide in cadmium stress tolerance in crop plants. Plant Physiology and Biochemistry **63**, 254–261.

Glass ADM, Erner Y, Kronzucker HJ, Schjoerring JK, Siddiqi MY, Wang MY. 1997. Ammonium fluxes into plant roots: energetics, kinetics, and regulation. Zeitschrift fur Pflanzenernahrung und Bodenkunde **160**, 261–268.

Guan MY, Zhu YX, Liu XX, Jin CW. 2019. Induction of S-nitrosoglutathione reductase reduces root cadmium uptake by inhibiting Iron-regulated transporter 1. Plant and Soil **438**, 251–262.

Gupta KJ, Fernie AR, Kaiser WM, van Dongen JT. 2011. On the origins of nitric oxide. Trends in Plant Science **16**, 160–168.

Hachiya T, Noguchi K. 2011. Integrative response of plant mitochondrial electron transport chain to nitrogen source. Plant Cell Reports **30**, 195–204.

Hachiya T, Watanabe CK, Fujimoto M, Ishikawa T, Takahara K, Kawai-Yamada M, Uchimiya H, Uesono Y, Terashima I, Noguchi K. 2012. Nitrate addition alleviates ammonium toxicity without lessening ammonium accumulation, organic acid depletion and inorganic cation depletion in *Arabidopsis thaliana* shoots. Plant & Cell Physiology **53**, 577–591.

Han M, Wu W, Wu WH, Wang Y. 2016. Potassium transporter KUP7 is involved in K^+ acquisition and translocation in *Arabidopsis* root under K^+-limited conditions. Molecular Plant **9**, 437–446.

Helenius A, Aebi M. 2001. Intracellular functions of N-linked glycans. Science **291**, 2364–2369.

Jadid N, Mialoundama AS, Heintz D, *et al.* 2011. DOLICHOL PHOSPHATE MANNOSE SYNTHASE1 mediates the biogenesis of isoprenyl-linked glycans and influences development, stress response, and ammonium hypersensitivity in *Arabidopsis*. The Plant Cell **23**, 1985–2005.

Jeandroz S, Wipf D, Stuehr DJ, Lamattina L, Melkonian M, Tian Z, Zhu Y, Carpenter EJ, Wong GK, Wendehenne D. 2016. Occurrence, structure, and evolution of nitric oxide synthase-like proteins in the plant kingdom. Science Signaling **9**, re2.

Kato H, Asai S, Yamamoto-Katou A, Yoshioka H, Doke N, Kawakita K. 2008. Involvement of *NbNOA1* in NO production and defense responses in INF1-treated *Nicotiana benthamiana*. Journal of General Plant Pathology **74**, 15–23.

Kempinski CF, Haffar R, Barth C. 2011. Toward the mechanism of NH_4^+ sensitivity mediated by *Arabidopsis* GDP-mannose pyrophosphorylase. Plant, Cell & Environment **34**, 847–858.

Krapp A. 2015. Plant nitrogen assimilation and its regulation: a complex puzzle with missing pieces. Current Opinion in Plant Biology **25**, 115–122.

Kronzucker HJ, Britto DT, Davenport RJ, Tester M. 2001. Ammonium toxicity and the real cost of transport. Trends in Plant Science **6**, 335–337.

Kronzucker HJ, Siddiqi MY, Glass ADM, Kirk GJD. 2000. Comparative kinetic analysis of ammonium and nitrate acquisition by tropical lowland rice: implications for rice cultivation and yield potential. New Phytologist **145**, 471–476.

Lay-Pruitt KS, Takahashi H. 2020. Integrating N signals and root growth: the role of nitrate transceptor NRT1.1 in auxin-mediated lateral root development. Journal of Experimental Botany **71**, 4365–4368.

Lee U, Wie C, Fernandez BO, Feelisch M, Vierling E. 2008. Modulation of nitrosative stress by S-nitrosoglutathione reductase is critical for

thermotolerance and plant growth in *Arabidopsis*. The Plant Cell **20**, 786–802.

Leitner M, Vandelle E, Gaupels F, Bellin D, Delledonne M. 2009. NO signals in the haze: nitric oxide signalling in plant defence. Current Opinion in Plant Biology **12**, 451–458.

Léran S, Edel KH, Pervent M, Hashimoto K, Corratgé-Faillie C, Offenborn JN, Tillard P, Gojon A, Kudla J, Lacombe B. 2015. Nitrate sensing and uptake in *Arabidopsis* are enhanced by ABI2, a phosphatase inactivated by the stress hormone abscisic acid. Science Signaling **8**, ra43.

Li BH, Li GJ, Kronzucher HJ, Baluška F, Shi WM. 2014. Ammonium stress in *Arabidopsis*: physiological targets, genetic loci, and signaling pathways. Trends in Plant Science **19**, 107–114.

Li B, Li Q, Xiong L, Kronzucker HJ, Krämer U, Shi W. 2012. *Arabidopsis* plastid AMOS1/EGY1 integrates abscisic acid signaling to regulate global gene expression response to ammonium stress. Plant Physiology **160**, 2040–2051.

Li B, Sun L, Huang J, Göschl C, Shi W, Chory J, Busch W. 2019. GSNOR provides plant tolerance to iron toxicity via preventing iron-dependent nitrosative and oxidative cytotoxicity. Nature Communications **10**, 3896.

Li B, Sun C, Lin X, Busch W. 2021. The emerging role of GSNOR in oxidative stress regulation. Trends in Plant Science **26**, 156–168.

Li G, Dong G, Li B, Li Q, Kronzucker HJ, Shi W. 2012. Isolation and characterization of a novel ammonium overly sensitive mutant, *amos2*, in *Arabidopsis thaliana*. Planta **235**, 239–252.

Li G, Li B, Dong G, Feng X, Kronzucker HJ, Shi W. 2013. Ammonium-induced shoot ethylene production is associated with the inhibition of lateral root formation in *Arabidopsis*. Journal of Experimental Botany **64**, 1413–1425.

Li Q, Li BH, Kronzucker HJ, Shi WM. 2010. Root growth inhibition by NH_4^+ in *Arabidopsis* is mediated by the root tip and is linked to NH_4^+ efflux and GMPase activity. Plant, Cell & Environment **33**, 1529–1542.

Liu L, Hausladen A, Zeng M, Que L, Heitman J, Stamler JS. 2001. A metabolic enzyme for S-nitrosothiol conserved from bacteria to humans. Nature **410**, 490–494.

Liu W, Li RJ, Han TT, Cai W, Fu ZW, Lu YT. 2015. Salt stress reduces root meristem size by nitric oxide-mediated modulation of auxin accumulation and signaling in *Arabidopsis*. Plant Physiology **168**, 343–356.

Liu Y, Lai N, Gao K, Chen F, Yuan L, Guo M. 2013. Ammonium inhibits primary root growth by reducing the length of meristem and elongation zone and decreasing elemental expansion rate in the root apex in Arabidopsis thaliana. PLoS One **8**, e61031.

Liu Y, von Wirén N. 2017. Ammonium as a signal for physiological and morphological responses in plants. Journal of Experimental Botany **68**, 2581–2592.

Lu Y, Zhang X, Jiang J, Kronzucker HJ, Shen W, Shi W. 2019. Effects of the biological nitrification inhibitor 1,9-decanediol on nitrification and ammonia oxidizers in three agricultural soils. Soil Biology & Biochemistry **129**, 48–59.

Malik SI, Hussain A, Yun BW, Spoel SH, Loake GJ. 2011. GSNOR-mediated de-nitrosylation in the plant defence response. Plant Science **181**, 540–544.

Matamoros MA, Cutrona MC, Wienkoop S, Begara-Morales JC, Sandal N, Orera I, Barroso JB, Stougaard J, Becana M. 2020. Altered plant and nodule development and protein S-nitrosylation in *Lotus japonicus* mutants deficient in S-nitrosoglutathione reductases. Plant & Cell Physiology **61**, 105–117.

Min J, Sun HJ, Kronzucker HJ, Wang Y, Shi WM. 2021. Comprehensive assessment of the effects of nitrification inhibitor application on reactive nitrogen loss in intensive vegetable production systems. Agriculture, Ecosystems and Environment **307**, 107227.

Neill SJ, Desikan R, Hancock JT. 2003. Nitric oxide signalling in plants. New Phytologist **159**, 11–35.

Peto A, Lehotai N, Feigl G, Tugyi N, Ördög A, Gémes K, Tari I, Erdei L, Kolbert Z. 2013. Nitric oxide contributes to copper tolerance by influencing ROS metabolism in *Arabidopsis*. Plant Cell Reports **32**, 1913–1923.

Qin C, Qian W, Wang W, Wu Y, Yu C, Jiang X, Wang D, Wu P. 2008. GDP-mannose pyrophosphorylase is a genetic determinant of ammonium sensitivity in *Arabidopsis thaliana*. Proceedings of the National Academy of Sciences, USA **105**, 18308–18313.

Royo B, Moran JF, Ratcliffe RG, Gupta KJ. 2015. Nitric oxide induces the alternative oxidase pathway in *Arabidopsis* seedlings deprived of inorganic phosphate. Journal of Experimental Botany **66**, 6273–6280.

Shabala L, Zhang J, Pottosin I, *et al.* 2016. Cell-type-specific H^+-ATPase activity in root tissues enables K^+ retention and mediates acclimation of barley (*Hordeum vulgare*) to salinity stress. Plant Physiology **172**, 2445–2458.

Shi HT, Li RJ, Cai W, Liu W, Wang CL, Lu YT. 2012. Increasing nitric oxide content in *Arabidopsis thaliana* by expressing rat neuronal nitric oxide synthase resulted in enhanced stress tolerance. Plant & Cell Physiology **53**, 344–357.

Shi H, Xiong L, Stevenson B, Lu T, Zhu JK. 2002. The *Arabidopsis* salt overly sensitive 4 mutants uncover a critical role for vitamin B6 in plant salt tolerance. The Plant Cell **14**, 575–588.

Simontacchi M, Galatro A, Ramos-Artuso F, Santa-María GE. 2015. Plant survival in a changing environment: the role of nitric oxide in plant responses to abiotic stress. Frontiers in Plant Science **6**, 977.

Straub T, Ludewig U, Neuhäuser B. 2017. The kinase CIPK23 inhibits ammonium transport in *Arabidopsis thaliana*. The Plant Cell **29**, 409–422.

Sun C, Lu L, Liu L, Liu W, Yu Y, Liu X, Hu Y, Jin C, Lin X. 2014. Nitrate reductase-mediated early nitric oxide burst alleviates oxidative damage induced by aluminum through enhancement of antioxidant defenses in roots of wheat (*Triticum aestivum*). New Phytologist **201**, 1240–1250.

Szczerba MW, Britto DT, Ali SA, Balkos KD, Kronzucker HJ. 2008*a*. NH_4^+-stimulated and -inhibited components of K^+ transport in rice (*Oryza sativa* L.). Journal of Experimental Botany **59**, 3415–3423.

Szczerba MW, Britto DT, Balkos KD, Kronzucker HJ. 2008*b*. Alleviation of rapid, futile ammonium cycling at the plasma membrane by potassium reveals K^+-sensitive and -insensitive components of NH_4^+ transport. Journal of Experimental Botany **59**, 303–313.

Szczerba MW, Britto DT, Kronzucker HJ. 2006. Rapid, futile K^+ cycling and pool-size dynamics define low-affinity potassium transport in barley. Plant Physiology **141**, 1494–1507.

Tanaka H, Maruta T, Ogawa T, Tanabe N, Tamoi M, Yoshimura K, Shigeoka S. 2015. Identification and characterization of *Arabidopsis* AtNUDX9 as a GDP-D-mannose pyrophosphohydrolase: its involvement in root growth inhibition in response to ammonium. Journal of Experimental Botany **66**, 5797–5808.

ten Hoopen F, Cuin TA, Pedas P, Hegelund JN, Shabala S, Schjoerring JK, Jahn TP. 2010. Competition between uptake of ammonium and potassium in barley and *Arabidopsis* roots: molecular mechanisms and physiological consequences. Journal of Experimental Botany **61**, 2303–2315.

Tian QY, Sun DH, Zhao MG, Zhang WH. 2007. Inhibition of nitric oxide synthase (NOS) underlies aluminum-induced inhibition of root elongation in *Hibiscus moscheutos*. New Phytologist **174**, 322–331.

Torralbo F, Menéndez S, Barrena I, Estavillo JM, Marino D, González-Murua C. 2017. Dimethyl pyrazol-based nitrification inhibitors effect on nitrifying and denitrifying bacteria to mitigate N_2O emission. Scientific Reports **7**, 13810.

Walker L, Boddington C, Jenkins D, *et al.* 2017. Changes in gene expression in space and time orchestrate environmentally mediated shaping of root architecture. The Plant Cell **29**, 2393–2412.

Wang C, Zhang SH, Li W, Wang PF, Li L. 2011. Nitric oxide supplementation alleviates ammonium toxicity in the submerged macrophyte *Hydrilla verticillata* (L.) Royle. Ecotoxicology & Environmental Safety **74**, 67–73.

Wang J, Yu Y, Zhang Z, Quan R, Zhang H, Ma L, Deng XW, Huang R. 2013. *Arabidopsis* CSN5B interacts with VTC1 and modulates ascorbic acid synthesis. The Plant Cell **25**, 625–636.

Wang L, Guo Y, Jia L, Chu H, Zhou S, Chen K, Wu D, Zhao L. 2014. Hydrogen peroxide acts upstream of nitric oxide in the heat shock pathway in *Arabidopsis* seedlings. Plant Physiology **164**, 2184–2196.

Wang ZH, Li SX. 2019. Nitrate N loss by leaching and surface runoff in agricultural land: a global issue (a review). Advances in Agronomy **156**, 159–217.

Wu X, Liu T, Zhang Y, Duan F, Neuhäuser B, Ludewig U, Schulze WX, Yuan L. 2019. Ammonium and nitrate regulate NH_4^+ uptake activity of *Arabidopsis* ammonium transporter AtAMT1;3 via phosphorylation at multiple C-terminal sites. Journal of Experimental Botany **70**, 4919–4930.

Xia J, Kong D, Xue S, *et al.* 2014. Nitric oxide negatively regulates AKT1-mediated potassium uptake through modulating vitamin B6 homeostasis in *Arabidopsis*. Proceedings of the National Academy of Sciences, USA **111**, 16196–16201.

Xiong J, Fu G, Tao L, Zhu C. 2010. Roles of nitric oxide in alleviating heavy metal toxicity in plants. Archives of Biochemistry and Biophysics **497**, 13–20.

Xu G, Fan X, Miller AJ. 2012. Plant nitrogen assimilation and use efficiency. Annual Review of Plant Biology **63**, 153–182.

Xu S, Guerra D, Lee U, Vierling E. 2013. S-nitrosoglutathione reductases are low-copy number, cysteine-rich proteins in plants that control multiple developmental and defense responses in *Arabidopsis*. Frontiers in Plant Science **4**, 430.

Yu M, Lamattina L, Spoel SH, Loake GJ. 2014. Nitric oxide function in plant biology: a redox cue in deconvolution. New Phytologist **202**, 1142–1156.

Yuan HM, Huang X. 2016. Inhibition of root meristem growth by cadmium involves nitric oxide-mediated repression of auxin accumulation and signalling in *Arabidopsis*. Plant, Cell & Environment **39**, 120–135.

Zhan N, Wang C, Chen L, *et al.* 2018. S-nitrosylation targets GSNO reductase for selective autophagy during hypoxia responses in plants. Molecular Cell **71**, 142–154.e6.

Zhang L, Li G, Wang M, Di D, Sun L, Kronzucker HJ, Shi W. 2018. Excess iron stress reduces root tip zone growth through nitric oxide-mediated repression of potassium homeostasis in *Arabidopsis*. New Phytologist **219**, 259–274.

Zhang X, Wang W, Kang X, Zhao L. 2020. *Arabidopsis* CaM3 inhibits nitric oxide accumulation and improves thermotolerance by promoting S-nitrosoglutathione reductase via direct binding. Plant Growth Regulation **90**, 41–50.

Zhao MG, Tian QY, Zhang WH. 2007. Nitric oxide synthase-dependent nitric oxide production is associated with salt tolerance in *Arabidopsis*. Plant Physiology **144**, 206–217.

Zheng X, He K, Kleist T, Chen F, Luan S. 2015. Anion channel SLAH3 functions in nitrate-dependent alleviation of ammonium toxicity in *Arabidopsis*. Plant, Cell & Environment **38**, 474–486.

Zhou S, Jia L, Chu H, Wu D, Peng X, Liu X, Zhang J, Zhao J, Chen K, Zhao L. 2016. *Arabidopsis* CaM1 and CaM4 promote nitric oxide production and salt resistance by inhibiting S-nitrosoglutathione reductase via direct binding. PLoS Genetics **12**, e1006255.

Zhu XF, Wang B, Song WF, Zheng SJ, Shen RF. 2016. Putrescine alleviates iron deficiency via NO-dependent reutilization of root cell-wall Fe in *Arabidopsis*. Plant Physiology **170**, 558–567.